

University of Nebraska - Lincoln

DigitalCommons@University of Nebraska - Lincoln

Virology Papers

Virology, Nebraska Center for

3-2-2023

Isolation and Characterization of a Novel Lytic Phage, vB_PseuP-SA22, and Its Efficacy against Carbapenem-Resistant *Pseudomonas aeruginosa*

Addisu D. Teklemariam

Rashad R. Al-Hindi

Mona G. Alharbi

Ibrahim Alotibi

Sheren A. Azhari

See next page for additional authors

Follow this and additional works at: <https://digitalcommons.unl.edu/virologypub>



Part of the [Biological Phenomena, Cell Phenomena, and Immunity Commons](#), [Cell and Developmental Biology Commons](#), [Genetics and Genomics Commons](#), [Infectious Disease Commons](#), [Medical Immunology Commons](#), [Medical Pathology Commons](#), and the [Virology Commons](#)

This Article is brought to you for free and open access by the Virology, Nebraska Center for at DigitalCommons@University of Nebraska - Lincoln. It has been accepted for inclusion in Virology Papers by an authorized administrator of DigitalCommons@University of Nebraska - Lincoln.

Authors

Addisu D. Teklemariam, Rashad R. Al-Hindi, Mona G. Alharbi, Ibrahim Alotibi, Sheren A. Azhari, Ishtiaq Qadri, Turki Alamri, Ahmed Esmael, and Steve Harakeh

Article

Isolation and Characterization of a Novel Lytic Phage, vB_PseuP-SA22, and Its Efficacy against Carbapenem-Resistant *Pseudomonas aeruginosa*

Addisu D. Teklemariam ¹, Rashad R. Al-Hindi ^{1,*}, Mona G. Alharbi ¹, Ibrahim Alotibi ², Sheren A. Azhari ¹, Ishtiaq Qadri ¹, Turki Alamri ³, Ahmed Esmael ^{4,5,*} and Steve Harakeh ^{6,*}

¹ Department of Biological Sciences, Faculty of Science, King Abdulaziz University, Jeddah 21589, Saudi Arabia

² Health Information Technology Department, Applied College, King Abdulaziz University, Jeddah 21589, Saudi Arabia

³ Family and Community Medicine Department, Faculty of Medicine in Rabigh, King Abdulaziz University, Jeddah 21589, Saudi Arabia

⁴ Botany and Microbiology Department, Faculty of Science, Benha University, Benha 13518, Egypt

⁵ Nebraska Center for Virology, University of Nebraska-Lincoln, Lincoln, NE 68583, USA

⁶ King Fahd Medical Research Center, Yousef Abdullatif Jameel Chair of Prophetic Medicine Application, Faculty of Medicine, King Abdulaziz University, Jeddah 21589, Saudi Arabia

* Correspondence: rhindi@kau.edu.sa (R.R.A.-H.); a7medesmael@gmail.com (A.E.); sharakeh@gmail.com (S.H.)



Citation: Teklemariam, A.D.; Al-Hindi, R.R.; Alharbi, M.G.; Alotibi, I.; Azhari, S.A.; Qadri, I.; Alamri, T.; Esmael, A.; Harakeh, S. Isolation and Characterization of a Novel Lytic Phage, vB_PseuP-SA22, and Its Efficacy against Carbapenem-Resistant *Pseudomonas aeruginosa*. *Antibiotics* **2023**, *12*, 497. <https://doi.org/10.3390/antibiotics12030497>

Academic Editors: Andrey A. Filippov and Mikeljon P. Nikolich

Received: 29 December 2022

Revised: 22 February 2023

Accepted: 27 February 2023

Published: 2 March 2023



Copyright: © 2023 by the authors. Licensee MDPI, Basel, Switzerland. This article is an open access article distributed under the terms and conditions of the Creative Commons Attribution (CC BY) license (<https://creativecommons.org/licenses/by/4.0/>).

Abstract: Carbapenem-resistant *Pseudomonas aeruginosa* (CRPA) poses a serious public health threat in multiple clinical settings. In this study, we detail the isolation of a lytic bacteriophage, vB_PseuP-SA22, from wastewater using a clinical strain of CRPA. Transmission electron microscopy (TEM) analysis identified that the phage had a podovirus morphology, which agreed with the results of whole genome sequencing. BLASTn search allowed us to classify vB_PseuP-SA22 into the genus *Bruynoghevirus*. The genome of vB_PseuP-SA22 consisted of 45,458 bp of double-stranded DNA, with a GC content of 52.5%. Of all the open reading frames (ORFs), only 26 (44.8%) were predicted to encode certain functional proteins, whereas the remaining 32 (55.2%) ORFs were annotated as sequences coding functionally uncharacterized hypothetical proteins. The genome lacked genes coding for toxins or markers of lysogenic phages, including integrases, repressors, recombinases, or excisionases. The phage produced round, halo plaques with a diameter of 1.5 ± 2.5 mm on the bacterial lawn. The TEM revealed that vB_PseuP-SA22 has an icosahedral head of 57.5 ± 4.5 nm in length and a short, non-contractile tail (19.5 ± 1.4 nm). The phage showed a latent period of 30 min, a burst size of 300 PFU/infected cells, and a broad host range. vB_PseuP-SA22 was found to be stable between 4–60 °C for 1 h, while the viability of the virus was reduced at temperatures above 60 °C. The phage showed stability at pH levels between 5 and 11. vB_PseuP-SA22 reduced the number of live bacteria in *P. aeruginosa* biofilm by almost five logs. The overall results indicated that the isolated phage could be a candidate to control CRPA infections. However, experimental in vivo studies are essential to ensure the safety and efficacy of vB_PseuP-SA22 before its use in humans.

Keywords: *Pseudomonas aeruginosa*; carbapenem resistance; bacteriophage; *Podovirus*; *Bruynoghevirus*; broad host range; anti-biofilm effect

1. Introduction

Pseudomonas aeruginosa (*P. aeruginosa*, PA) is a Gram-negative bacterium involved in opportunistic infections in humans. *P. aeruginosa* is the main cause of nosocomial infections, which can result in the demise of those infected, especially among immunosuppressed patients with severe wounds, chronic obstructive lung disease, cystic fibrosis, ventilator-associated pneumonia, and catheter-associated chronic urinary tract infections. Some

P. aeruginosa strains cause life-threatening infections due to their capability to form biofilms and their natural and/or acquired drug resistance [1–3].

It has been long established that antibiotics play a crucial role in healthcare, food processing, agriculture, veterinary medicine, and many other industries. Nevertheless, the overuse and misuse of antibiotics have caused bacteria to evolve escape mechanisms and become resistant to the majority of antibiotics [4,5]. Furthermore, the shortage of new antibiotics developed over the past few years has left us with very limited therapeutic agents against pathogenic bacteria. Antibiotic resistance has been predicted to cause 10 million deaths annually by 2050 [4,6].

Antibiotics such as carbapenems have been launched for the treatment of serious *P. aeruginosa* infections. These antibiotics are considered the last line of treatment against diseases caused by multidrug-resistant (MDR) Gram-negative bacteria [7]. As carbapenems are the last therapeutic option for the control of bacterial infections, carbapenem-resistant *P. aeruginosa* (CRPA) has become a serious public health threat in several clinical settings [8]. Therefore, *P. aeruginosa* has been classified as a ‘Priority 1 critical pathogens by WHO, for which new antibacterial is urgently required’ [9].

Biofilms are formed as a network of microbial communities, protecting the microbes from any external damage while providing mechanical stability and adhesion to surfaces [10]. Bacterial biofilms can resist antibiotics due to impaired diffusion of the antibiotics, selection of resistant mutants, antibiotic efflux, oxygen and nutrient limitation, expression of biofilm-specific genetic mechanisms, or survival of tolerant cells [11]. The ability of microbial biofilms to resist host immunity, as well as antibiotics, is the main cause of persistent infections [11].

P. aeruginosa biofilms are significant virulence factors and may influence chronic wound healing, especially in diabetic patients with non-healing ulcers on their lower extremities, as well as chronic burn wound infections [12]. Biofilms of *P. aeruginosa* bacteria are especially deadly in patients with cystic fibrosis [13]. The biofilm protects the microbial organisms from disinfectants as well as antibiotics, maintaining their survival on biotic and abiotic surfaces [14]. *P. aeruginosa* forms thick biofilms due to the production of large quantities of alginate, a polysaccharide that consists of D-mannuronate and L-guluronate units. Compared to the planktonic forms, the biofilm form of *P. aeruginosa* can exhibit >100-fold greater resistance to conventional antibiotics [15,16].

In a previous study using a mouse model of early lung infection, researchers observed collateral damage in healthy cells associated with the induction of neutrophils in response to *P. aeruginosa* biofilms. This occurred through a phenomenon called “frustrated phagocytosis,” with the surrounding healthy host tissues being attacked by the toxins secreted by activated phagocytic cells [17].

Currently, available antibiotics may reduce the bacterial population in biofilms; however, they cannot fully eliminate the biofilm [18,19], and therefore, relapses of biofilm infections may occur. Hence, amputation of infected tissues or removal of implanted materials, as well as successive durable antimicrobial therapy, might be required to terminate the biofilm-associated infections. Furthermore, new treatments aimed at eradicating biofilms are needed; in this context, bacteriophages could provide an interesting possible alternative [16,20,21]. In terms of biofilm eradication, phages present fascinating characteristics, as they encode enzymes that enable them to directly penetrate and destroy biofilms. Depolymerases are phage-encoded enzymes that specifically destroy exopolysaccharide matrix components, preventing their formation by distracting the quorum-sensing network and enhancing the penetration of the phage [22]. These enzymes are commonly found as structural proteins such as baseplates and tail fibers but may also exist as soluble proteins during the replication cycle. They are involved in the initial attachment to the host cell surface and the destruction of the bacterial capsule to facilitate the phage infection process [15].

Phage therapy, which denotes the bacteriophage-based treatment of bacterial infections, could provide a helpful therapeutic approach for fighting infections caused by

multidrug-resistant *P. aeruginosa* infections [23–25]. Knowledge about the potential therapeutic phages is vital for the development of phage therapy. Nevertheless, phages are not frequently used therapeutically due to various constraints, such as inadequate clarity of phage formulations, the narrow specific spectrum of activity, poor viability or stability of phage preparations, and a lack of understanding of the mechanism of action of phages and their heterogeneity [26,27]. Despite these constraints, the global increase in MDR pathogenic bacteria has led to the revival of interest in phage-based therapeutic approaches [23].

Phage therapy against *P. aeruginosa* biofilms has been assessed in both in vivo and in vitro studies. For instance, phage PELP20 showed a 3-log phage reduction of biofilm in a mouse model of cystic fibrosis infection [28]. Similarly, a temperate phage Φ Pan70 significantly reduced *P. aeruginosa* biofilm production in a mouse model [29]. In another study, the combined use of Φ MR299-2 and Φ NH-4 eliminated the biofilm and killed *P. aeruginosa* growing in the cystic fibrosis bronchial epithelial CFBE41o-cell line. In in vitro experiments, bacteriophages such as M-1, PB1-like, phiKZ-like, and LUZ24-like phages have been shown to be effective in destroying the planktonic cells as well as the biofilm [30,31].

Despite the above-mentioned reports, very limited lytic bacteriophages have been characterized against CRPA infections so far [32]. Hence, this study was conducted to isolate and characterize a lytic bacteriophage targeting CRPA. In addition, the anti-biofilm effect of the isolated phage was investigated.

2. Materials and Methods

2.1. Bacterial Strains and Culture Condition

The clinical strain of CRPA (*P. aeruginosa* strain B10) was obtained from King Abdulaziz University hospital and used as a host for the isolation of vB_PseuP-SA22 from wastewater. Identification of the organism was carried out using an API 20 E test kit (bioMérieux Industry, Hazelwood, MO, USA), a VITEK identification system (bioMérieux Inc., Durham, NC, USA) using GN ID REF21341 cards, and 16S rRNA molecular analysis and sequencing. The bacterial strains used to evaluate the host range of vB_PseuP-SA22 are listed in Table 1. Some of these isolates were obtained from the King Fahd Medical Research Center (KFMRC), while the others were purchased from American Type Culture Collection (ATCC). All bacterial isolates used in our study were preserved using 25% glycerol at $-20\text{ }^{\circ}\text{C}$ until used.

2.2. Antibiotic Sensitivity Test

Antimicrobial susceptibility was assessed using the standard agar disk diffusion method following the CLSI guideline (Supplementary Table S1). *P. aeruginosa* ATCC 27853 was used as a positive control [33].

2.3. Enrichment and Isolation of Bacteriophages

To isolate potential lytic bacteriophages, we collected wastewater samples from Jeddah Wastewater Treatment Plant, Saudi Arabia. The samples were transported to the KFMRC laboratory on ice, stored at $4\text{ }^{\circ}\text{C}$, and processed within 24 h. The wastewater samples were centrifuged at $10,000\times g$ for 10 min, and the supernatant was passed through $0.22\text{ }\mu\text{m}$ filters (Fischer Scientific, Ottawa, ON, Canada) to remove unnecessary particulates (including bacterial cells) and debris. The filtrate was then directly used for phage isolation [34]. Briefly, 20 mL of the filtrate was added to 20 mL of an overnight culture of CRPA in double-strength nutrient broth supplemented with 2 mM CaCl_2 . The culture was placed in a shaking incubator with gentle shaking (100 rpm) at $37\text{ }^{\circ}\text{C}$ for 48 h. Afterward, it was centrifuged at $6000\times g$ for 12 min at $4\text{ }^{\circ}\text{C}$, and the supernatant was filtered using $0.22\text{ }\mu\text{m}$ size filters to exclude host bacteria and contaminants. Finally, the filtrates were stored at $4\text{ }^{\circ}\text{C}$ until further use.

Table 1. Host range of vB_PseuP-SA22 against *P. aeruginosa* and other bacterial species.

Bacterial Strains	Antibiotic Resistance Profile	Plaque Assay
<i>P. aeruginosa</i> ATCC 27853	NR	+
<i>P. aeruginosa</i> strain M19	MDR	+
<i>P. aeruginosa</i> PA14	MDR	+
<i>P. aeruginosa</i> (Clinical isolate)	MDR	+
<i>P. aeruginosa</i> (Clinical isolate)	MDR	+
<i>P. aeruginosa</i> (Clinical isolate)	MDR	+
<i>P. aeruginosa</i> strain DW1 (Environmental isolate)	MDR	+
<i>P. aeruginosa</i> strain N155 (Environmental isolate)	XDR	-
<i>P. aeruginosa</i> strain YUSA1 (Environmental isolate)	XDR	-
<i>P. aeruginosa</i> (Environmental isolate)	XDR	-
<i>P. aeruginosa</i> (Environmental isolate)	MDR	+
<i>Escherichia coli</i> strain NRC129	ESBLs	+
<i>Escherichia coli</i> strain NBRC 102203-68	ESBLs	+
<i>Escherichia coli</i> strain E24	ESBLs	+
<i>Staphylococcus aureus</i>	NR	-
Methicillin-resistant <i>Staphylococcus aureus</i> ATCC 43330	MDR	-
<i>Salmonella enterica</i> subsp. <i>enterica</i> serovar Typhimurium strain FDAARGOS_321	MDR	-
<i>S. typhimurium</i> strain CUB 32/10	MDR	-
<i>S. waycross</i> strain SA20041608	MDR	-
<i>S. arizonae</i> serovar 62:z4,z23	MDR	-
<i>S. enteritidis</i> strain FORC_052	MDR	-
<i>Enterococcus</i> sp. strain B43	NR	-
Bacterium BEL C6	NR	-

ESBLs, Extended-spectrum beta-lactamases producer; XDR, extensively drug-resistant; NR, non-antibiotic resistant strain.

2.4. Spot Assay

The presence of phage in the lysate was determined by spot assay [35]. In brief, 0.1 mL of exponential phase host culture was mixed with 4 mL of molten soft agar (0.7% *w/v* agar), then poured on the surface of nutrient agar plates to create a lawn. Thereafter, 5 µL of the crude phage extract was spotted on top of the soft agar and kept in a laminar airflow for 20 minutes to allow for viral adsorption. The inoculated plate was incubated overnight at 37 °C. The sample was considered positive for phage if it produced a clear inhibition (lytic) zone.

2.5. Purification

Purification of the phage was carried out through a double-layer agar assay (DLA), as described elsewhere [36]. Briefly, typical phage plaques were picked up from the soft agar layer by touching the top layer using a 1 mL pipette tip and transferred into 500 µL sterile PBS (pH 7.4) suspension. The suspension was then kept at 4 °C overnight for proper diffusion of phages from the soft agar. Thereafter, 10-fold serial dilutions of the purified lysates were conducted, and DLA assay was carried out to quantify the phage titer and

the uniformity of the plaques. The purification process was repeated until similar plaques were obtained. The purified lysate was stored at 4 °C.

2.6. Concentration of Phages

A full-plate lysate method was used to increase the titer of bacteriophages, following the technique detailed in [37,38]. Confluent lysis zone was produced in the top agar overlay, and 8 mL of PBS was poured over the top agar. Then, the plate was kept at 4 °C overnight for proper diffusion of the virions from the soft agar into PBS. Thereafter, the suspension was aspirated with a 10 mL sterile syringe and transferred into a test tube. The collected suspension was then centrifuged at $8000 \times g$ for 5 min, and the supernatant was passed through 0.22 µm filters to eliminate bacterial debris. The purified phage lysate was then used to determine the titer of phage using the DLA technique.

2.7. Bacteriophage Titer Determination

The purified phage lysate was diluted 10-fold in PBS solution and plated using the DLA technique. The plaques on each plate were individually counted. To calculate the phage titer, we used the last plate, which had plaque counts ranging from 30–300. The titer was calculated, and the results were recorded as PFU mL⁻¹ [39]. The size of the plaque was measured using a ruler, and photographs were captured using a digital camera.

2.8. Stability of *P. aeruginosa* Phage

2.8.1. Thermal Stability

The thermal stability test was conducted according to Jurczak-Kurek et al. with slight modifications [40]. Briefly, micro-centrifuge tubes containing a mixture of 100 µL of the purified phage lysate (1×10^8 FU/mL) and 900 µL PBS (pH 7.4) were incubated in a water bath at different temperatures (4 °C, 40 °C, 50 °C, 60 °C, 70 °C, 80 °C, or 90 °C) for 1 h. Phage suspended in an equal volume of PBS (pH 7.5) kept at 4 °C was used as a control. Then, the phage titer after treatment was determined by the DLA method. This experiment was carried out in triplicate.

2.8.2. Phage pH Stability Test

The pH stability of the vB_PseuP-SA22 was tested as described elsewhere, with minor adjustments [41]. The pH of fresh/sterile nutrient broth (pH 2–14) was adjusted, using a pH meter, by adding 1 M HCl and NaOH drop by drop. Nine milliliters of pH-adjusted medium was mixed with 1 mL of phage suspension and incubated at 37 °C for 1 h. Then, the titers of vB_PseuP-SA22 in each suspension were determined using the DLA method. This experiment was carried out in triplicate.

2.9. Bacterial Reduction Assay

The in vitro host reduction ability of vB_PseuP-SA22 was assessed as described elsewhere, with minor modifications [42]. Briefly, 100 µL of *P. aeruginosa* culture (OD 0.4, 10^7 CFU/mL) was added to 100 µL of diluted isolated phage (10^4 – 10^9 PFU/mL) in microtiter plate wells. Thus, 0.001, 0.01, 0.1, 1, 10, and 100 multiplicities of infection (MOI) were generated. The bacterial reduction potential was measured by DLA at different time intervals over 48 h. Bacterial culture without phage (OD 0.4) was used as a control (100 µL of bacterial culture mixed with 100 µL of fresh nutrient broth). The results are presented as mean values ± SD from three independent experiments, and the bacterial reduction curve (CFU/mL vs. time) was also plotted.

2.10. Determination of Optimal Multiplicity of Infection (MOI)

The bacterial cultures in the exponential phase were washed away with PBS three times and adjusted to analogous concentrations of 10^6 , 10^7 , 10^8 , 10^8 , 10^8 , and 10^8 CFU/mL, then the phages and bacteria were mixed with MOIs of 100, 10, 1, 0.1, 0.01, and 0.001, respectively. Thereafter, the suspension was incubated for 2 h at 37 °C, and the titer of phages was carried

out by the DLA method [43]. The optimal MOI was determined according to the ratio of the specified titer (PFU/mL) of phages to the specified concentration of host bacteria (CFU/mL); in particular, the MOI value attaining the highest phage titer was considered the optimal MOI.

2.11. Phage Adsorption Assay

The adsorption rate of phages onto the surface of host cell was assessed based on a formerly used protocol [44]. The exponential phase bacterial culture was collected and re-suspended in sterile nutrient broth to reach an OD₆₀₀ of 0.4. Then, the phage was added at an MOI of 0.1, and the adsorption was monitored at 37 °C for 90 min. One milliliter aliquot was collected at regular time intervals and centrifuged (10,000 × g, 10 min). The supernatant was filtrated using a 0.22 µm pore-size filter. The titers of the phage in the original phage stock (t₀) and supernatant (t₁) were determined by the DLA technique. The adsorption rate was estimated as (t₀ – t₁)/t₀.

2.12. One-Step Growth Curve

A cycle growth pattern test was performed using vB_PseuP-SA22 and its host bacteria in order to investigate the latent period and the burst size, as described by others, with minor modifications [35]. Briefly, the experiment was initiated at an MOI of 0.1 in a sterile centrifuge tube containing phage (1 × 10⁷ PFU/mL) and its host strains (1 × 10⁸ CFU/mL) in 10 mL nutrient broth. The mixture was placed in a shaker incubator and incubated at 37 °C for 10 min for proper adsorption of phage onto the host cell surface. Afterward, the suspension was centrifuged at 12,000 × g for 10 min. After removing the supernatant, the pellet of infected cells was mixed with 10 mL of pre-warmed nutrient broth and incubated in a shaker incubator (120 rpm) at 37 °C. Thereafter, 100 µL of sample was collected at 10-min intervals over a period of 60 min. To determine the phage titers, we diluted aliquots with PBS (pH 7.4), and the soft agar overlying technique was used. The time difference between adsorption (excluding the first 20 min of pre-incubation) and the initial point of the first burst was considered as the latent period, and the ratio of the end count of progeny virions to the number of infected bacterial cells found at the initial point during the latent period was considered as the burst size.

2.13. Host Spectrum

The host range of vB_PseuP-SA22 was determined by a spot assay, as described elsewhere [45], using a panel of 23 species of bacteria with different antimicrobial sensitivity profiles (Table 1). Briefly, 5 µL of the isolated phage (10⁹ PFU/mL) was dropped onto the lawn of the tested species. Then, after overnight incubation at 37 °C, the presence of plaques (lytic zones) on the spotted area was determined to be positive, whereas the absence of any lytic zone was considered negative for the test. Positive results were further confirmed by the DLA method.

2.14. Transmission Electron Microscopy (TEM)

The morphology of vB_PseuP-SA22 was determined by TEM. The purified phage lysate (1 × 10⁹ PFU/mL) was placed onto thin carbon films, and the adsorbed phages were negatively stained with 2% (w/v; pH 5.0) uranyl acetate [46]. The virions were observed using a TEM 910 (Carl Zeiss, Oberkochen, Germany) at 80 kV. The morphology of the virions was captured using a Slow-Scan CCD-Camera (ProScan, 1024 × 1024, Scheuring, Germany). Certain parameters, such as the head and tail length of the virion, were measured twice using the ImageJ software. The identification guidelines indicated by the International Committee of Taxonomy of Viruses were implemented to assess the phenotypic diversity of the virion [47].

2.15. Biofilm Formation and Reduction Assay

2.15.1. Test Tube Biofilm Production Assay

The biofilm production capacity of CRPA was determined according to the tube biofilm production method (TM) described by Di Domenico et al. (2016) [48]. The test organism was first inoculated in a polystyrene test tube which contained nutrient broth, then incubated at 37 °C for 24 h. Next, the planktonic cells found in all tubes were discarded and rinsed twice with PBS. Thereafter, the emptied polystyrene tubes were stained with 0.1% crystal violet (CV; HiMedia Labs Pvt. Ltd., Dindori, Nashik, India) for 1 h. Then, after air-drying, if stained visible film lined the inside walls, the bottom of the tube was considered to be positive for biofilm production. A biofilm-negative culture of *Escherichia coli* (*E. coli*) was used as a negative control.

2.15.2. Microtiter Plate Biofilm Production and Reduction Assay

The anti-biofilm activity of vB_PseuP-SA22 was assessed in optically clear, flat-bottom 96-well plates (SPL, Pocheon, Korea), in accordance with the methods stated by Fong et al. [49], with slight modifications. Briefly, the overnight grown culture (1×10^7 cells/mL) was inoculated into the sterile nutrient broth, following which aliquots (200 μ L) were distributed to individual wells. Two different microplates, one for staining and another for enumeration of bacteria, were then incubated at 37 °C for 12 h with slight shaking (120 rpm). The supernatant of each individual well was discarded and rinsed twice with PBS (pH 7.4) to eliminate all planktonic cells, followed by treatment with 200 μ L of phage suspension (1×10^6 PFU/mL) for 4, 8, and 12 h. The plates were then washed twice with PBS and air-dried. The number of bacterial cells in the biofilm was enumerated by re-suspending the biofilm in PBS after scraping the well with a sterile pipette tip, following which the suspension was diluted and plated. The total biomass of the biofilm was quantified by staining with CV (0.1%, *w/v*) for 15 min, and the wells were then rinsed with PBS. CV was dissolved in an acetone–ethanol solution (20:80, *v/v*), and the intensity of CV staining (OD value) was quantified at 595 nm using a Plate Reader Infinite 200 pro (MTX Lab Systems, Austria) [49]. This assay was repeated three times. The OD values higher than the control or blank well were considered to indicate biofilm producers.

2.16. Scanning Electron Microscopy

Scanning electron microscopy (SEM) was conducted at KFMRC in order to assess the biofilm reduction potential of vB_PseuP-SA22, following a previously described method [50,51]. Biofilms were grown on a glass coverslip initially placed into a 96-well microtiter plate, then rinsed twice with PBS and dried in a bacteriological incubator at 37 °C for 20 h. The mounted biofilms were fixed with glutaraldehyde (2.5%) and dehydrated continuously with different concentrations of ethanol (30–100%) for 5 min in each. Thereafter, they were sputtered with gold, and the status of the biofilms was examined using SEM (SEM; Norcada Inc., Edmonton, AB, Canada).

2.17. Extraction of Bacteriophage DNA

The DNA of the concentrated phage (1×10^{12} PFU/mL) was extracted using a phage DNA extraction kit (QIAGEN, Germany) based on the instructions provided by the manufacturers. The concentration and purity of the extracted DNA were assessed using a spectrophotometer (Invitrogen Qubit) and examined by agarose gel electrophoresis [52].

2.18. Whole-Genome Sequence and Bioinformatic Analysis

Sequencing of the vB_PseuP-SA22 genomic DNA was performed at the Pittsburgh genome sequencing center (USA) using an Illumina HiSeq platform. The sequence output was assembled using ABySS v2.0.2, and the resulting contigs were assembled using the assembly algorithm Newbler version 3.0, with default parameters. RAST and GeneMark were used to predict and annotate potential open reading frames. The circular map was built using the CGView online tool, and the GC content and GC skew of the genome were

assessed accordingly [53]. We used the PHIRE platform to generate promoters specific to the vB_PseuP-SA22 DNA sequence [54]. The ARNOLD online tool was used to identify the number and types of Rho-factor independent terminators [55]. GeneMarks [56] and PHAST were employed to locate the open reading frames (ORFs) [57]. The function of each coding sequence was predicted by the protein basic local alignment search tool (Blastp) of the NCBI server [58]. GtRNAdb and tRNA Scan-SE tools were used to predict putative tRNAs [59,60]. The existence of allergic proteins in the predicted coding sequences was also inspected using the food and allergy search tool. Finally, the existence of virulence factors was assessed by ResFinder and the virulence factor database (VFDB) [61,62].

2.19. Phylogenetic Analysis

Nucleotide sequence alignment was performed using ClustalW, and the resulting aligned sequence was used to construct the phylogenetic tree using the MAFFT v.7 software. During the construction of the tree, the neighbor-joining method and 1000 bootstrap replicates were applied [63,64].

2.20. Comparative Genomic Analysis

The comparative genomic sequence was conducted using the circleto program, and a circular ideogram was built according to a method described elsewhere [65].

2.21. Statistical Analysis

The data were recorded as means \pm SE of triplicate experiments. The statistical analysis was conducted using two-way analysis of variance (ANOVA). We used version 6 of the GraphPad Prism software to perform the analyses. The significance level was set at $p < 0.05$.

2.22. Nucleotide Sequence Accession Number

The sequence data for the *P. aeruginosa* phage vB_PseuP-SA22 was deposited in the GenBank under accession number OP793496.

3. Results

3.1. Identification of the Host Bacteria and Its Antibiotic Sensitivity Profile

The host bacteria were identified phenotypically by API 20 (Supplementary Figure S3) and Vitek (Supplementary Table S3) and further characterized at the molecular level, with 16S rRNA sequence analysis carried out for confirmation. The BLAST nucleotide similarity search revealed that the used CRPA showed 99% sequence similarity to *P. aeruginosa* deposited in the national database (Accession: JQ900545.1).

The sensitivity of *P. aeruginosa* strain B10 to common conventional antibiotics was determined in accordance with the CLSI guidelines (Supplementary Table S1). The strain was resistant against 93.8% of the tested antibiotics, including aminoglycosides (amikacin, tobramycin, streptomycin, neomycin, and gentamicin), second- and third-generation cephalosporins (cefuroxime, cefotaxime, ceftriaxone, and ceftazidime), fluoroquinolones (levofloxacin and ciprofloxacin), and carbapenems (meropenem, ertapenem, and imipenem), but not to colistin (Figure 1).

3.2. Phage Isolation and Morphology

We isolated a novel wastewater phage, vB_PseuP-SA22, using CRPA *P. aeruginosa* strain B10 as a host. The isolated phage produced round, halo plaques of 1.5 ± 2.5 mm in diameter on a lawn of the host cells (Figure 2B). The TEM results revealed that vB_PseuP-SA22 had an icosahedral head of 57.5 ± 4.5 nm in length and had a short, non-contractile tail (19.5 ± 1.4 nm). It was found to have a podophage morphology (Figure 2C).

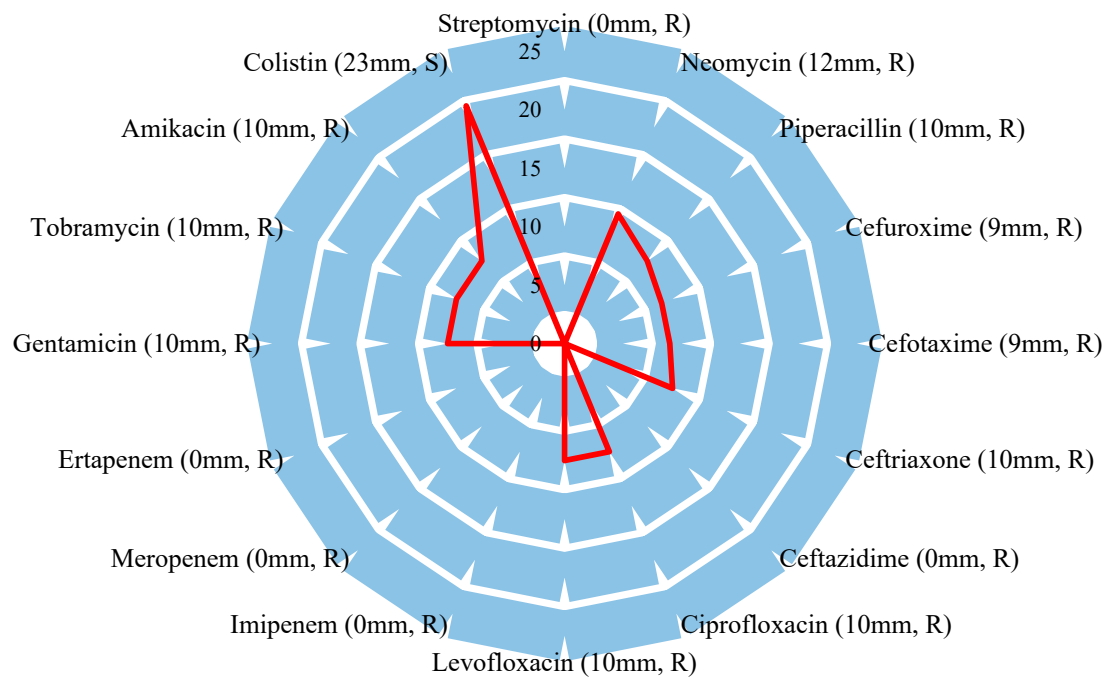


Figure 1. Radar plot showing the antibiotic resistance profile of *P. aeruginosa* strain B10. R = resistant, S = sensitive. The size of the inhibition zone is presented in mm; 0 mm indicates no inhibition zone detected (i.e., the tested bacterium was not sensitive to the respective antibiotic).

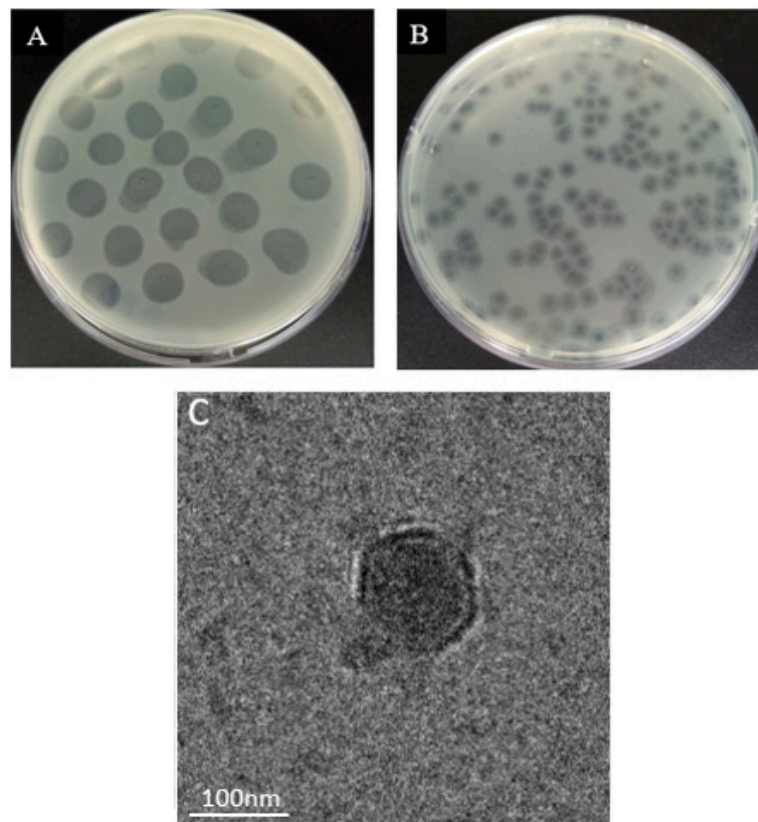


Figure 2. (A) Spot assay (lytic zone on the lawn of *P. aeruginosa* strain B10); (B) typical vB_PseuP-SA22 plaques; and (C) transmission electron micrograph of vB_PseuP-SA22 under negative staining with 2% uranyl acetate. The size of petri plates = 90 mm; bar = 100 nm.

3.3. Phage Adsorption Assay and One-Step Growth Curve

The rate of adsorption of the vB_PseuP-SA22 phage on the host cell surface is presented in Figure 3A. The virions attached to the host bacterial cell surface quickly, and 60% had adsorbed at 20 min post-infection. Nearly all virions were attached to the surface of the host cells at 23 min post-infection (Figure 3A).

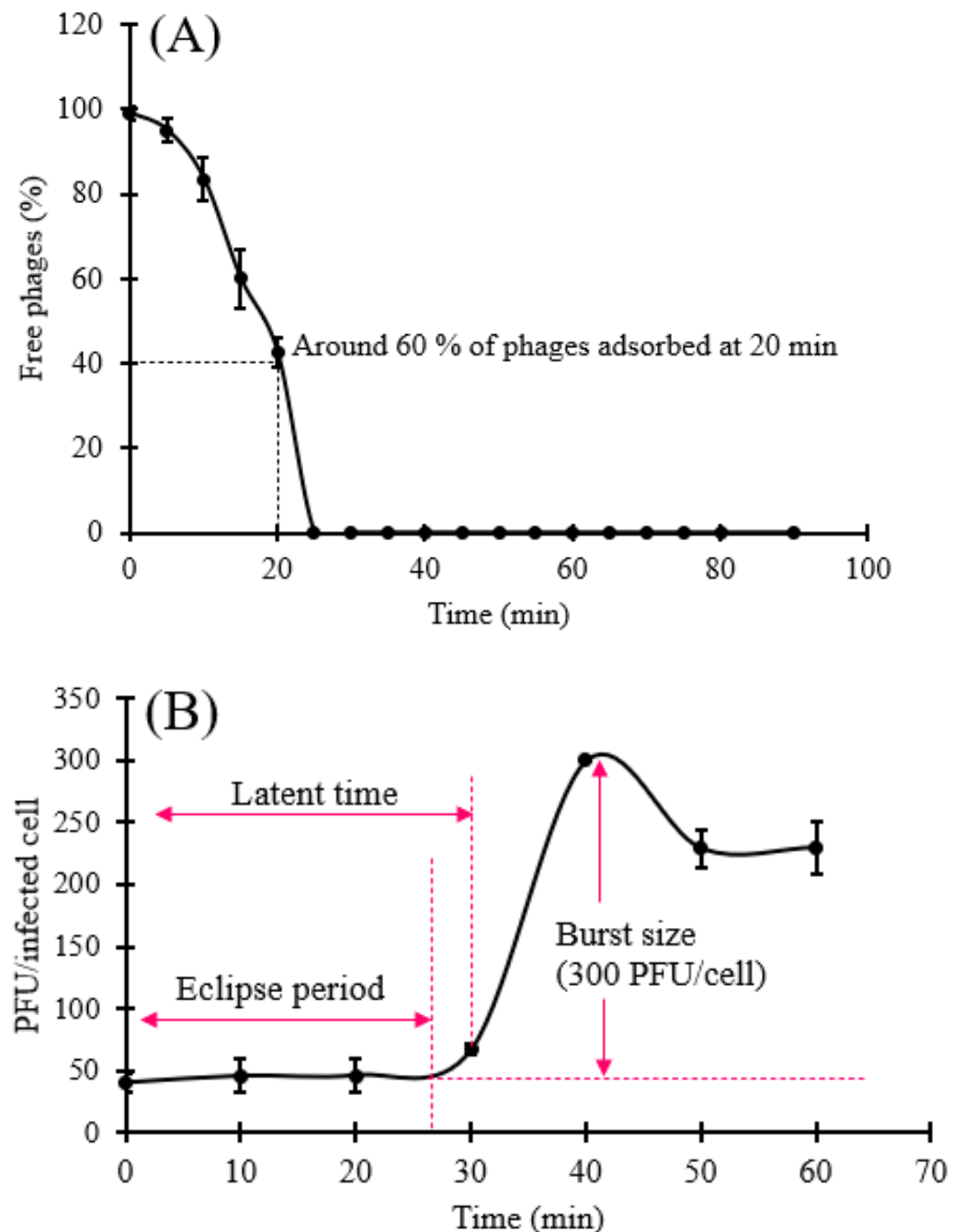


Figure 3. (A) Phage adsorption plots of vB_PseuP-SA22. The X-axis represents the time of exposure and Y-axis indicates the percentage of free phage particles found at different time points. (B) Three phases of one round lytic cycle of vB_PseuP-SA22. All values represent the mean \pm SD of triplicated experiments.

A one-step growth experiment was carried out to assess the burst size and the latent period of vB_PseuP-SA22. The growth pattern indicated that the latent period of vB_PseuP-

SA22 was roughly 30 min, and the mean burst size was found to be 300 PFU/infected cell (Figure 3B).

3.4. Stability Test and Bacterial Challenge Test

The temperature stability assessment indicated that vB_PseuP-SA22 was stable between 4–60 °C for 1 h, while the viability of the virus was reduced at temperatures over 60 °C. The approximate titer was $8 \log_{10}$ PFU/mL upon incubation at 4 °C, 37 °C, 40 °C, 50 °C, or 60 °C for 1 h, and no significant differences ($p > 0.05$) were noticed in this temperature range. Nevertheless, we noticed that the thermal resistance rate declined to roughly $5.35 \log_{10}$ PFU/ml ($p < 0.05$) at 70 °C, and the phage fully lost viability at 80 °C, as shown in Figure 4A.

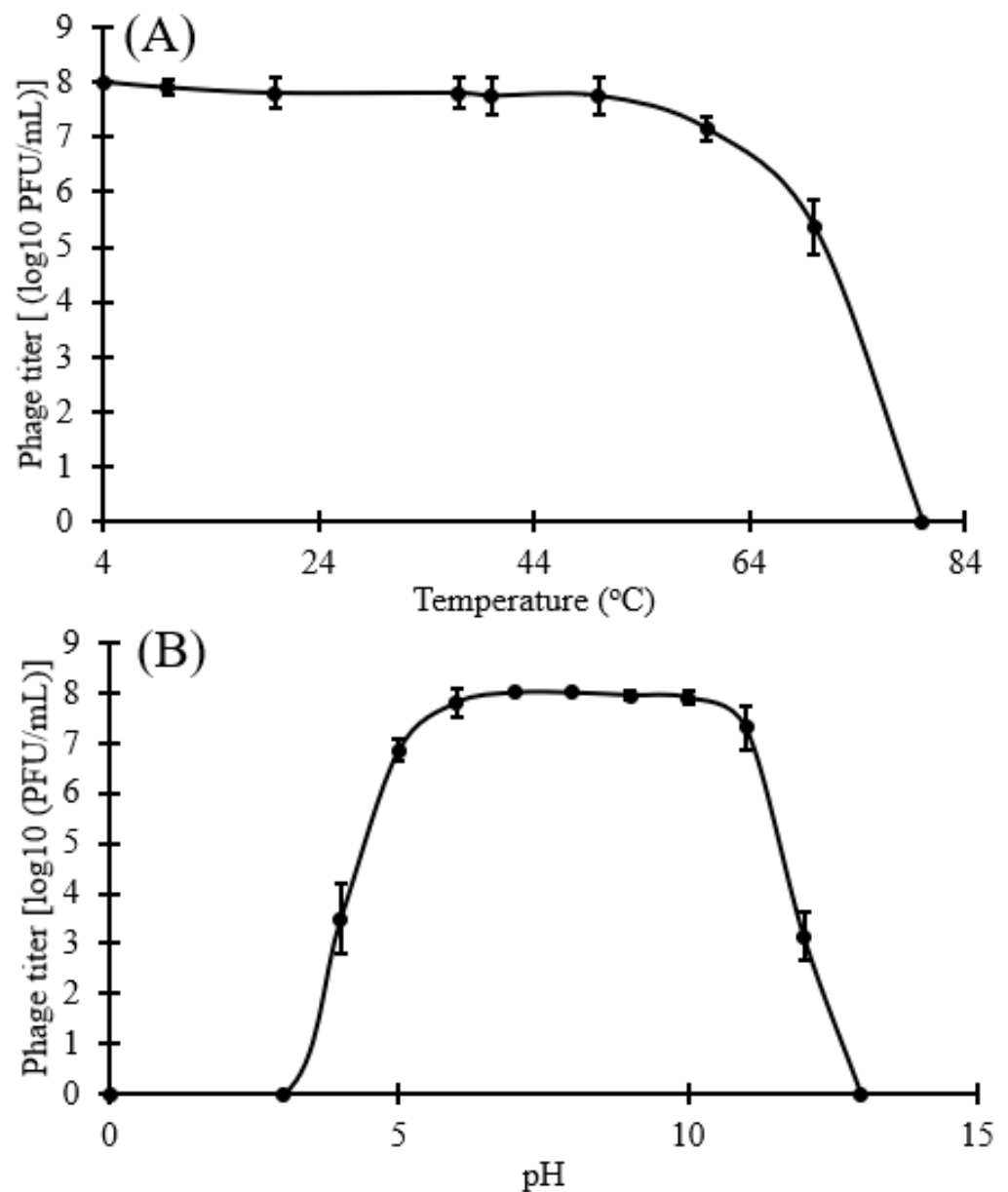


Figure 4. Cont.

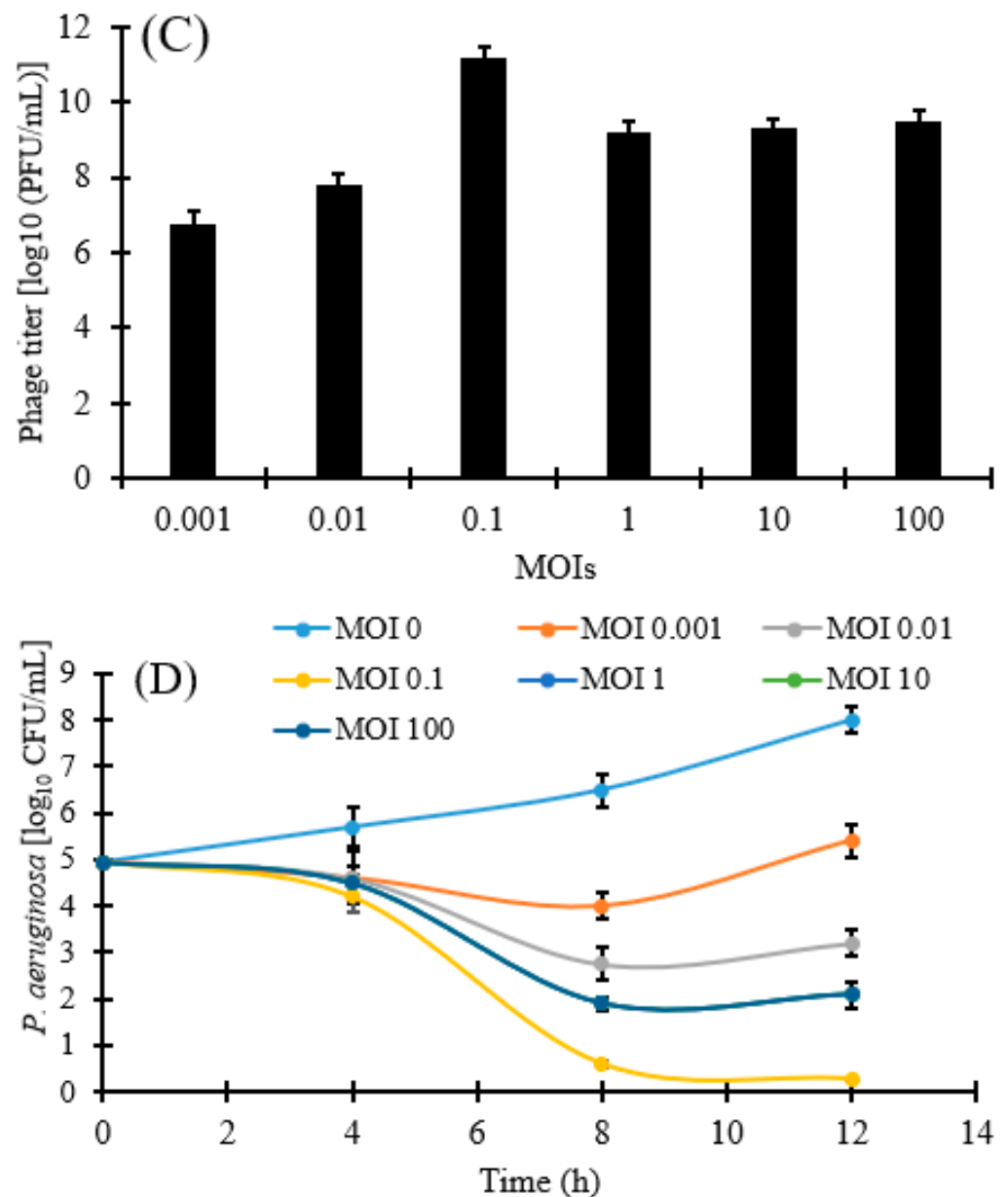


Figure 4. (A) Stability of vB_PseuP-SA22 under thermal treatment; (B) pH stability of vB_PseuP-SA22; (C) Determination of optimal MOI; and (D) Lysis kinetics. Error bars represent mean value \pm SD. Two-way ANOVA and the Bonferroni post-hoc test were conducted using the GraphPad Prism software. Significant statistical differences were noted between the control and the respective phage-treated samples at different MOIs ($p < 0.05$).

The pH stability test results indicated that the activity of vB_PseuP-SA22 was relatively stable at pH values between 5 and 11; in particular, vB_PseuP-SA22 retained approximately $8 \log_{10}$ PFU/mL from pH 5–11 for 1 h. Nevertheless, it displayed a significant reduction ($p < 0.05$) in titer at pH 4 and 12, with titers of 3.5 and $3.15 \log_{10}$ PFU/mL, respectively. Furthermore, vB_PseuP-SA22 was inactivated at $\text{pH} \leq 2$ and $\text{pH} \geq 12$. pH 7 and 8 were found to be the optimal pH values for vB_PseuP-SA22 (Figure 4B).

The lysis kinetics of vB_PseuP-SA22 were determined at different MOIs (100, 10, 1, 0.1, 0.01, and 0.001). Based on two-way ANOVA tests, significant differences were observed for all MOIs in comparison to the control (0 MOI; $p < 0.05$). As shown in Figure 4D, the density of bacteria in the untreated control increased by $\sim 3.05 \log$ CFU/mL at 12 h of incubation. The highest reduction in the concentration of live bacteria, by $4.67 \log_{10}$ CFU/mL at 12 h,

was recorded at an MOI of 0.1 compared to the original concentration ($p < 0.05$). Similar reductions (by approximately $2.85 \log_{10}$ CFU/mL) were observed at MOIs of 1, 10, and 100.

3.5. Host Range

The spectrum of lytic activity of vB_PseuP-SA22 was assessed by spot assay and confirmed by DLA. To do this, we used a phage stock with a titer of 1×10^8 PFU/mL against a panel of 23 bacterial strains (Table 1). The results revealed that vB_PseuP-SA22 showed lytic activity against 47.8% ($n = 11$) of tested bacterial strains, including 8/11 (72.7%) of *P. aeruginosa* strains (Table 1). These results, therefore, indicated that vB_PseuP-SA22 has a broad host range.

3.6. Genomic Analysis of the vB_PseuP-SA22 Phage Genome

Whole-genome sequence analysis revealed that the genome of vB_PseuP-SA22 was 45,458 bp (45.5 Kb) in length, with a GC content of 52.5% (Figure 5). Using Artemis and BLAST analysis, 58 ORFs were predicted as protein-coding sequences (CDSs) transcribed in both directions. Of the 58 putative ORFs, 32 ORFs were on the negative strand, while the other 26 ORFs were on the positive strand. Among the total encoding sequences, only 26 (44.8%) ORFs were found to encode the products homologous to proteins with known function, while 32 (55.2%) ORFs were annotated as hypothetical proteins (Supplementary Table S2). Twenty-six ORFs were predicted as functional proteins by BLASTP and RAST analyses, distributed in the following major functional groups: head-associated proteins (ORF4, ORF6, ORF7, ORF8, ORF22), tail-associated proteins (ORF14, ORF32, ORF13), DNA replication and regulation proteins (ORF27, ORF31, ORF37, ORF38, ORF45, ORF30), protein biosynthesis (ORF40, ORF42), packaging proteins (ORF24, ORF25, ORF26, ORF3), other proteins (ORF10, ORF20, ORF21, ORF18, ORF19), and a host cell lysis protein (ORF33); see Table 2.

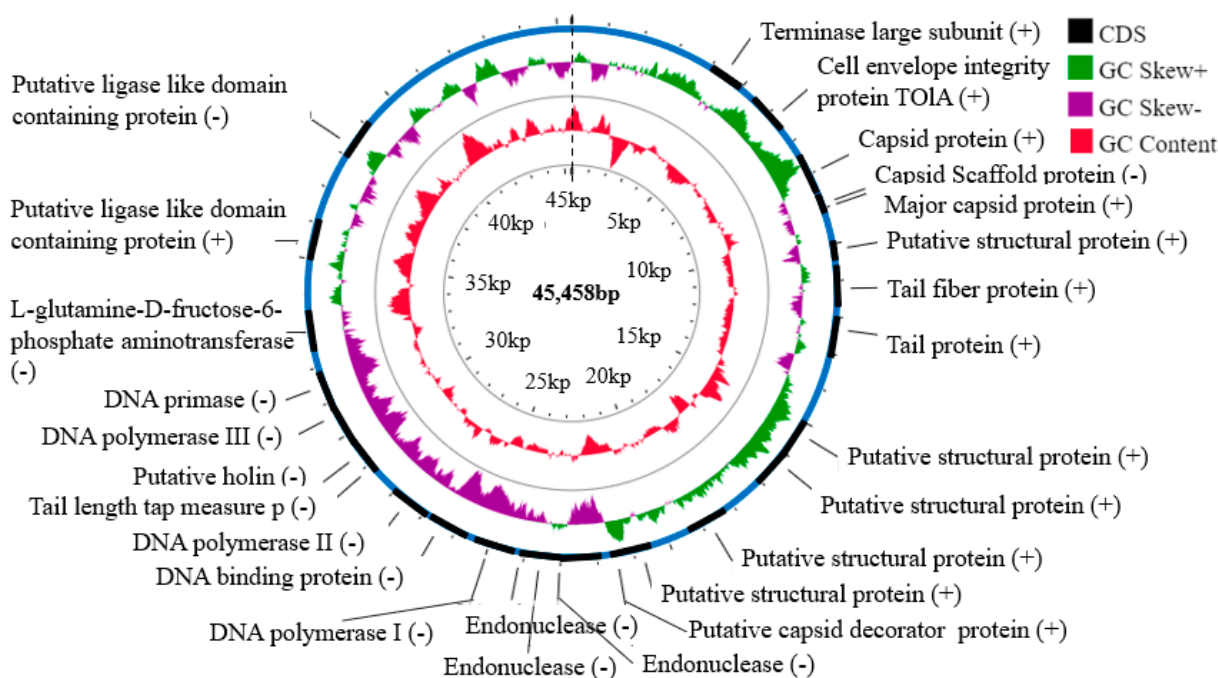


Figure 5. Circular genome map of vB_PseuP-SA22. The outer circle designates the ORFs of vB_PseuP-SA22. The red inner landscape shows the GC content, while the second inner circle with the purple and green landscape shows the GC skew. The CDSs with identified functions are labeled in black color, along with their location, while other unlabeled CDSs (blue) represent hypothetical proteins. The direction of the functional CDCs is represented as (+) for the main strand and (-) for the complementary strand. Scale units are base pairs.

Table 2. The annotated functional ORFs of vB_PseuP-SA22.

ORFs	Coverage	Length	Direction	Functions	Categories
ORF #4	5149–7266	2118	Forward	Cell envelope integrity protein TolA	Head-associated proteins
ORF #6	7511–8503	993	Forward	Putative capsid and scaffold protein	
ORF #7	8402–9361	960	Reverse	Capsid and scaffold protein	
ORF #8	8522–9475	954	Forward	Major capsid protein	
ORF #22	21,287–21,643	357	Forward	Putative capsid decoration protein	Tail-associated proteins
ORF #14	11,554–13,095	1542	Forward	Tail protein	
ORF #32	28,635–29,144	510	Reverse	Tail-length tape measure protein	
ORF #13	10,898–11,545	648	Forward	Tail fibers protein	
ORF #27	24,550–25,434	885	Reverse	DNA polymerase I	DNA replication and regulation proteins
ORF #31	26,795–28,273	1479	Reverse	DNA polymerase II	
ORF #37	30,360–30,869	510	Reverse	DNA polymerase III	
ORF #38	30,853–32,094	1242	Reverse	DNA primase	
ORF #45	37,796–38,803	1008	Forward	Putative ligase-like domain-containing protein	
ORF #30	26,171–26,725	555	Reverse	DNA-binding protein	
ORF #40	32,940–33,338	399	Reverse	Putative glutamyl-tRNA amidotransferase	Protein biosynthesis
ORF #42	34,578–36,110	1533	Reverse	Putative L-glutamine-D-fructose-6-phosphate amidotransferase	
ORF #24	22,642–23,403	762	Reverse	Putative endonuclease	Packaging proteins
ORF #25	23,396–23,746	351	Reverse	Putative endonuclease	
ORF #26	23,628–24,575	948	Reverse	Endonuclease	
ORF #3	3700–5148	1449	Forward	Terminase large subunit	
ORF #33	29,221–29,508	288	Reverse	Putative holin	Cell lysis
ORF #10	9848–10,474	627	Forward	Putative structural protein	Other structural proteins
ORF #20	17,204–20,374	3171	Forward	Putative structural protein	
ORF #21	20,268–21,272	1005	Forward	Putative structural protein	
ORF #18	15,137–15,520	384	Forward	Putative structural protein	
ORF #19	15,525–17,048	1524	Forward	Putative structural protein	

The genome of vB_PseuP-SA22 was identified to be linear, as it was cleaved by the exonuclease *Bal31*, which degrades only double-stranded linear DNA from both ends simultaneously. It does not comprise genes coding for recombinases, integrases, excisionases, or repressors, which are the chief markers of lysogenic bacteriophages. Hence, we confirmed that our isolate was likely an obligate lytic phage following only a lytic cycle. Additionally, no genes were found that encode virulence factors, as assessed by testing against the VFDB. Thus, the results suggest that vB_PseuP-SA22 meets multiple requirements of a safe and virulent phage and, therefore, is a candidate for use in treating *P. aeruginosa*-associated infections.

3.7. Predicted tRNA and Rho-Independent Transcription Terminators

A total of three tRNAs were predicted using the tRNAscan-SE de facto tool. They were asparagine (Asn), aspartic acid (Asp), and proline (Pro) tRNAs with GTT, GTC, and TGG

anti-codons, respectively (Table 3). The predicted tRNAs were situated at different locations in the whole genomic sequence with the specified isotype score (Supplementary Figure S2).

Table 3. Genomic characteristics of the predicted tRNAs.

tRNA#	tRNA Begin–End	tRNA Type	Anti-Codon	Introns Begin	Bounds End	Inf Score	Isotype CM	Score
1	2461–2533	Asn	GTT	0	0	64.0	Thr	57.6
2	2541–2613	Asp	GTC	0	0	64.3	Thr	65.2
3	2713–2786	Pro	TGG	0	0	70.6	Arg	72.9

A total of eight rho-independent terminators were predicted by ARNold (RNAmotif and/or Erpin tool). The terminators were composed of loops and stems located at different regions of the genomic sequence (Supplementary Figure S1).

3.8. Phylogenetic Analysis

Phylogenetic analyses of vB_PseuP-SA22 were conducted using BLASTn in comparison to the reference phage sequences deposited in a public database (NR, NCBI), and the tree was constructed using MEGA software. The whole-genome phylogenetic analysis indicated that the isolated phage showed high homology with *Pseudomonas* phages that belong to the family *Podoviridae*, genus *Bruynoghevirus*, as shown in Figure 6A. It had 96%, 94%, and 90% similarity with 95%, 98%, and 74% query coverage with *Pseudomonas* phages PSA16 (MZ089733.1), SaPL (MH973725.1), and Epa1 (MT108723.1), respectively. This suggests that vB_PseuP-SA22 also belongs to the family *Podoviridae*, genus *Bruynoghevirus*. Similarly, the constructed phylogenetic analysis relying on the terminase large sub-units indicated that the upper five phages classified under the *Podoviridae* family—namely, *Pseudomonas* phage phiPA01_302, *Pseudomonas* phage oldone, *Pseudomonas* phage U47, *Pseudomonas* virus Pa22, and *Pseudomonas* phage vB_PaeP_C2-10_Ab22—showed higher sequence similarity than the other phages classified under the same family (Figure 6B).

3.9. Comparative Genomic Analysis

Comparative genomic analysis was performed using the circoletto program in order to determine the sequence similarity between the selected four *Pseudomonas* phage genomes and vB_PseuP-SA22. Each quadrant represents an individual genome, and the ribbons connecting genomes represent local alignments produced by BLAST (Figure 7). The high sequence similarity is represented by red, followed by orange and blue colors. The results revealed that all four BLAST sequences displayed high-level sequence similarity to the query phage sequence (vB_PseuP-SA22).

3.10. Biofilm Production

In the first experiment, the test tube ring assay technique was used to assess the biofilm production capacity of *P. aeruginosa* strain B10. In this assay, the overnight culture of planktonic bacteria was gently removed, and the remaining biofilm (Supplementary Figure S4A,B) was stained using crystal violet and thus visualized, as shown in Supplementary Figure S4C. The three polystyrene test tubes inoculated with *P. aeruginosa* strain B10 produced a white clump on the inner wall of the test tube, which was stained violet. These results indicated that the organism was positive for biofilm production. Similarly, in the second experiment, biofilm production was assessed and quantified using a microtiter plate assay. The round violet rings on the inner wall and the bottom of the microtiter plate were indicative of biofilm production.

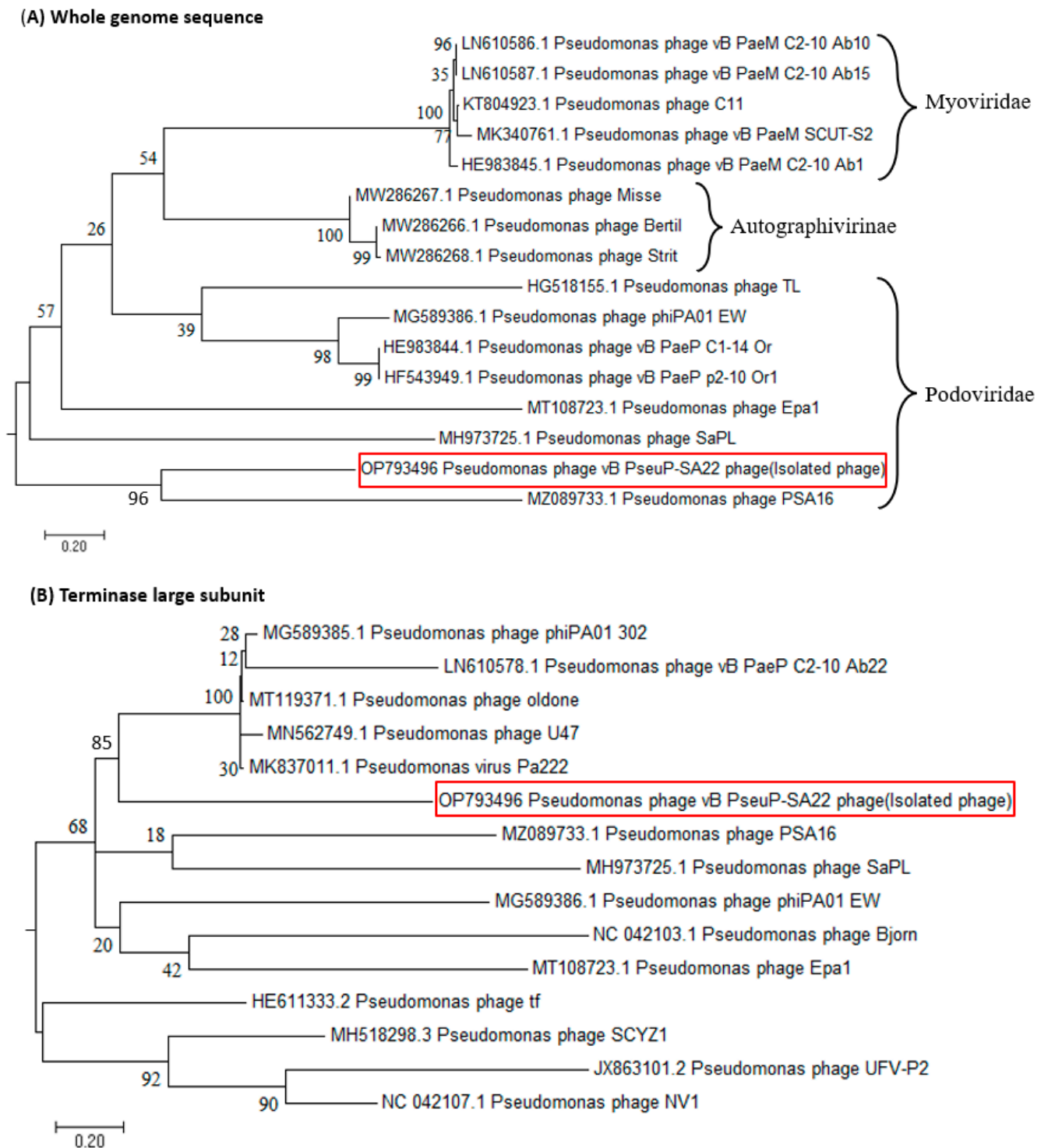


Figure 6. Neighbor-joining phylogenetic trees based on (A) whole-genome sequence and (B) terminase large sub-unit of vB_PseuP-SA22. The red color indicates the position of vB_PseuP-SA22. Reference phage sequences were obtained from the above-mentioned databases.

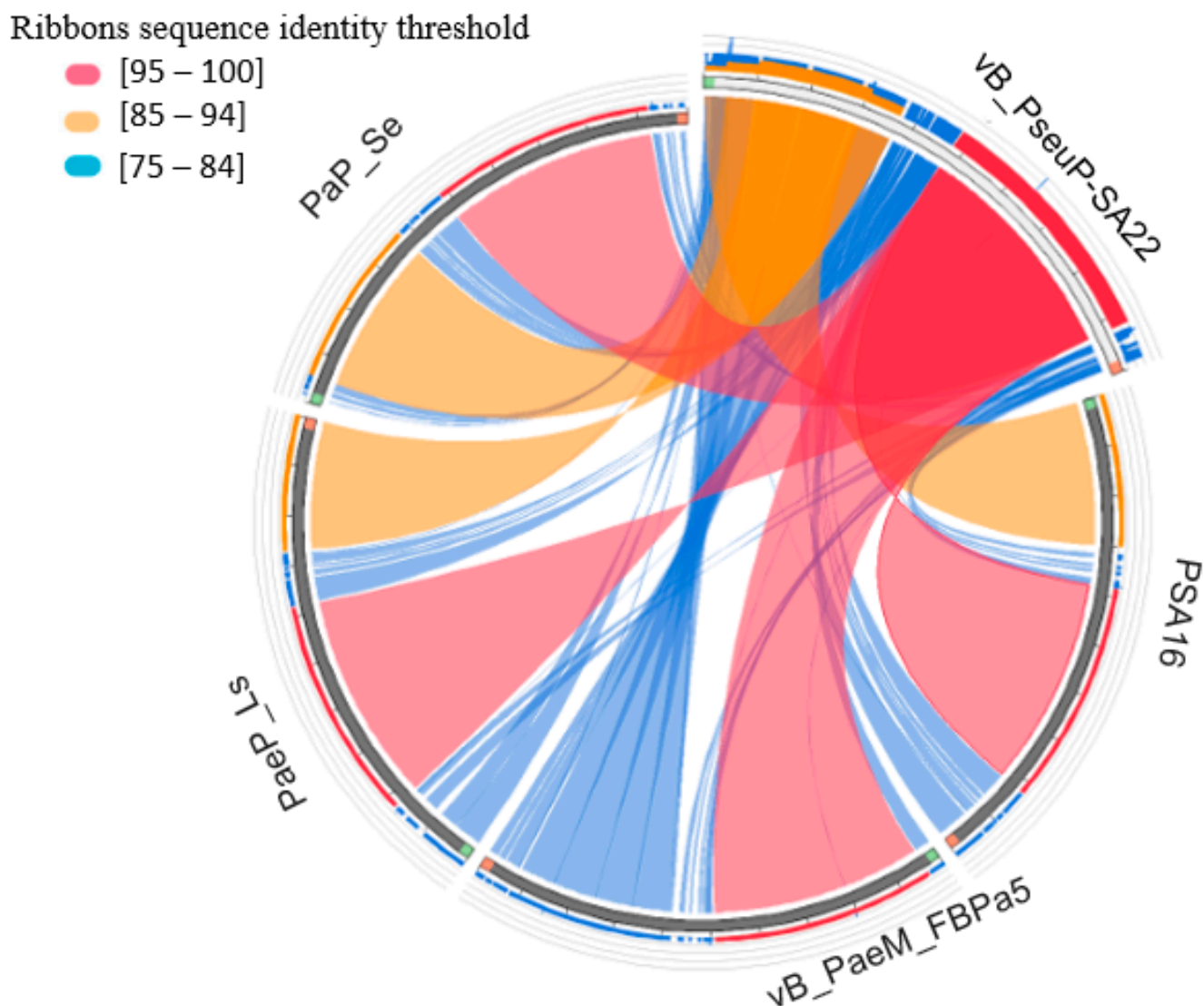


Figure 7. Circos plot showing the whole-genomic comparison of five *Pseudomonas* phages (including vB_PseuP-SA22) in five different quadrants. The colored ribbons found inside the circle denote the local BLAST alignments, representing the different levels of the maximum score, as indicated in the legend.

3.11. Biofilm Reduction Assay

The anti-biofilm activity of vB_PseuP-SA22 was assessed in 96-well plates, as described in Materials and Methods (Figure 7A). The results revealed that the anti-biofilm activity of vB_PseuP-SA22 was noticeable at an MOI of 0.1. The total biomass of biofilm showed a significant reduction ($p < 0.001$) at 4, 8, and 12 h. The viable bacterial cell count inside the biofilm was also significantly reduced ($p < 0.001$) throughout the incubation period, resulting in 2.25, 1.25, 0.34, and 0 \log_{10} CFU/mL at 0, 4, 8, and 12 h, respectively (Figure 8B). Scanning electron microscopic images also confirmed the total disruption of pre-formed biofilms at 12 h of treatment with phage vB_PseuP-SA22, as shown in Figure 8C.

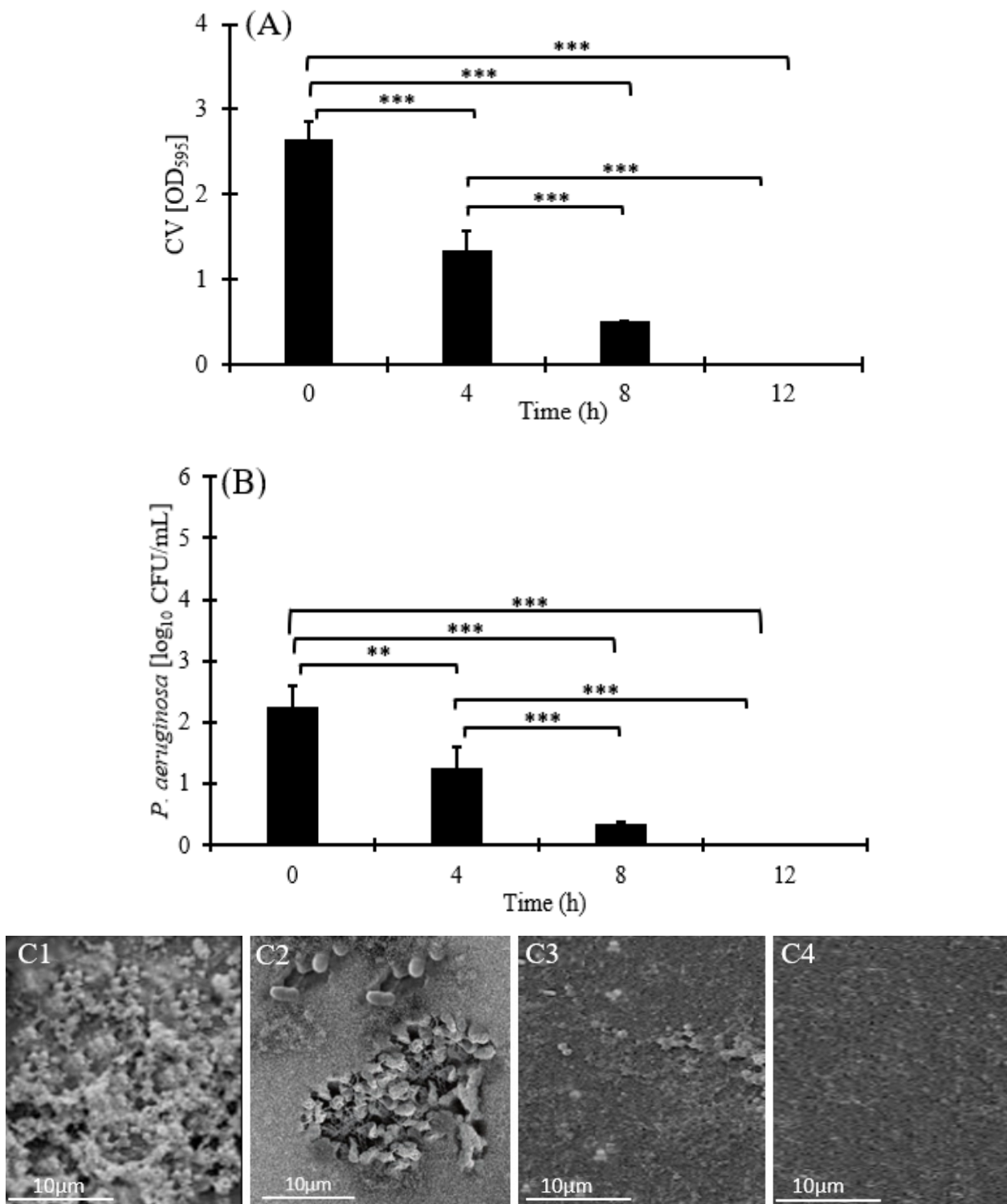


Figure 8. (A) Anti-biofilm activity of vB_PseuP-SA22 on biofilms of CRPA at an MOI of 0.1. (B) Viable bacterial cell counts at different ages of biofilm at an MOI of 0.1. All values designate mean \pm SD of triplicate experiments. Two-way ANOVA and the Bonferroni post-hoc test were carried out using the GraphPad Prism software. Significant differences are illustrated using asterisks ($p < 0.05$; **, $p < 0.01$; ***, $p < 0.001$); and (C1–C4) Scanning electron microscopic images showing the biofilm at different time intervals (C1, 0 h; C2, 4 h; C3, 8 h; C4, 12 h). Scale bar = 10 μ m at a magnification of 5000 \times .

4. Discussion

At present, nosocomial pathogens such as *P. aeruginosa* pose a serious public health threat worldwide due to their resistance to a variety of antimicrobial agents [66]. According to a study conducted by the World Health Organization in 2016, CRPA was ranked second among 20 antimicrobial-resistant bacterial species for which new antibacterials are urgently required [9]. To date, scientists and clinicians all over the globe have worked intensively to find promising alternative antimicrobial approaches (e.g., phage therapy) and combinatorial therapies [67,68]. Phage therapy against *Pseudomonas* spp. has considerably improved over the past decade [69]. Nevertheless, little is known regarding CRPA-specific phages [32].

In this study, we isolated a phage with potential lytic ability against CRPA from wastewater. vB_PseuP-SA22 has an icosahedral head and short, non-contractile tail, which is typical of podophages. Similar reports have indicated that multiple phages active against MDR *P. aeruginosa* were isolated from wastewater in different geographical locations [31,70]. Wastewater, in general, comprises a wide variety of micro-organisms due to contamination from fecal and hospital wastes [71], and wastewater is a good source of phages against multiple antibiotic-resistant bacterial strains [72].

The whole-genome sequence of the vB_PseuP-SA22 revealed that its genome is a 45,458 bp long double-strand DNA sequence with 56 ORFs. The genome does not carry any harmful genes, such as those linked with lysogeny, antibiotic resistance, toxins, or other factors associated with the virulence of the host bacterium. This suggests that vB_PseuP-SA22 can be considered as a virulent phage, a potential therapeutic agent against CRPA. The lysis cassette of vB_PseuP-SA22 encodes for holin (encoded by ORF35). Holin is a small phage-encoding protein that incorporates into the cell membrane, forms large holes and transports endolysin across the membrane [73]. Phages likely lyse cells to release their progeny through the holin–endolysin lytic system, which is common within almost all dsDNA phages [74]. The vB_PseuP-SA22 genome encodes for three tRNAs. There is evidence suggesting that lytic phages contain a greater number of tRNAs than temperate phages [75]. Most temperate phages (e.g., *E. coli* phage P4, P22, or Lambda) lack tRNA genes. Phages play a major role in horizontal gene transfer within bacteria. tRNA genes, however, are crucial housekeeping genes that are expected to be least susceptible to lateral gene transfer [76]. When these genes are deleted, rates of protein synthesis and burst sizes are lowered. Yet, why some phages possess tRNAs remains a mystery [77].

The stability of phages in a wide range of thermal and pH conditions is known to be a very crucial factor for the optimal replication of the viral particle in the host bacteria [78]. According to this study, vB_PseuP-SA22 displayed stability in a pH range of 4.0 to 12. Extreme basic or acidic pH could considerably influence the infectivity of most phages, and researchers have suggested that these situations cause the denaturation of phage proteins and, subsequently, loss of their viability [79]. Previous works have verified that most tailed phages are stable in a pH range of 5.0 to 9.0 [80,81], similar to the results obtained in this study.

A spot assay was employed to determine the host range of the isolated phage. However, the clear zone created in the tested bacterial strains sometimes is associated with bacteriocins, which might be present in the prepared suspension [82]. Hence, the spot assay result was further confirmed by plaque assay. In this line, vB_PseuP-SA22 was found to be lytic for a broad range of bacterial strains tested.

The bacterial killing assay indicated that the highest growth rate was recorded at an MOI of 0.1. On the other hand, normal growth was observed without phage (control), and the cell concentration kept increasing steadily throughout the incubation period. Bacterial reduction assay is one of the principal factors in determining the applicability of newly isolated phages to be used in phage therapy. The lytic kinetics showed a radical decline in bacterial growth from 4 to 8 h post-infection. However, except for 0.1 MOI, a slight increase in bacterial growth was noticed at all the other MOIs. According to previous reports, this result may be due to the development of phage-resistant mutants following infection; this characteristic is regarded as a drawback of phage therapy [83].

The biofilm reduction assay indicated that administration of vB_PseuP-SA22 led to a significant reduction ($p < 0.001$) in the biofilm biomass. In this assay, the growth of the host bacteria found in the biofilm was also significantly reduced ($p < 0.001$). Guo et al. have reported that two *Myoviridae* phages, vB_PaeM_SCUT-S1 (S1) and vB_PaeM_SCUT-S2 (S2), inhibited the growth of the *P. aeruginosa* strain PAO1 at low MOI levels, and showed good performance both in eradicating pre-formed biofilms as well as in preventing biofilm formation [84]. Similarly, in a study by Vukotic et al. [85], the *A. baumannii* phage ISTD produced 2 and 3.5 log reductions in a biofilm-associated bacterial cell and planktonic cell count, respectively [85]. In another study, five *P. aeruginosa* phages isolated from domestic sewage showed good performance regarding the degradation of biofilms formed in the endotracheal tubes [86]. A high biofilm reduction potential has been reported by Yuan et al. when using the anti-*P. aeruginosa* phage vB_PaeM_LS1 at 8 h post-infection [87]. Latz et al. have reported that three phages—phiKZ-like, PB1-like, and LUZ24-like—suppressed the biofilm as well as the planktonic form of MDR *P. aeruginosa* [30].

Several studies have indicated that the antibiofilm activity of phages is mainly associated with the enzymes that they encode. Polysaccharide depolymerases are phage-encoded polysaccharide-degrading enzymes that are highly specific and mainly associated with the tail structure of the virions, such as tail spikes, tail fibers, tail tubular, or base plate proteins [88]. They have a specific binding site with respect to capsular polysaccharides, lipopolysaccharides, or exopolysaccharides of the host bacteria. According to a recent report by Knecht et al., the biofilms of *P. aeruginosa* can be destabilized by alginate-specific tail spike proteins [15].

5. Conclusions

In conclusion, we successfully isolated a lytic bacteriophage targeting CRPA from samples collected from a wastewater treatment plant in Jeddah, Saudi Arabia. vB_PseuP-SA22 presented a wide host range and remained active in a wide range of temperatures and pH conditions. Its high burst size, a lack of toxic, virulent, and/or antibiotic-resistant genes in its genome, together with its antibiofilm activity against the tested host strain, are all crucial features of vB_PseuP-SA22, demonstrating its promise as an alternative therapeutic agent in treating infections associated with multidrug-resistant *P. aeruginosa* infections. Therefore, further clinical studies and other comprehensive in vivo examinations are necessary to investigate the therapeutic properties of the isolated phage against MDR *P. aeruginosa*. In addition, the combined effect of vB_PseuP-SA22 with other lytic bacteriophages may also be assessed in order to optimize its use.

Supplementary Materials: The following supporting information can be downloaded at: <https://www.mdpi.com/article/10.3390/antibiotics12030497/s1>, Table S1: Antibiotic disks used to test *P. aeruginosa* and their respective concentrations; Table S2: Annotated open reading frame (58 CDC) of vB_PseudoP-SA22; Table S3: Vitek 2 identification results; Figure S1: Genomic feature of the predicted rho-independent terminators; Figure S2: Predicted tRNA structures; Figure S3: API-20E test results; Figure S4: Photographs showing qualitative detection of biofilm production.

Author Contributions: Conceptualization, A.D.T., R.R.A.-H. and S.H.; methodology, A.D.T. and A.E.; software, M.G.A.; validation, A.D.T., R.R.A.-H. and A.E.; formal analysis, I.A.; investigation, S.A.A.; resources, A.D.T. and R.R.A.-H.; data curation, I.Q. and T.A.; writing—original draft A.D.T. and A.E.; review and editing, R.R.A.-H., I.Q., T.A. and S.H. visualization, I.A.; supervision, R.R.A.-H., I.Q., A.E. and S.H.; project administration, R.R.A.-H. and S.H.; funding acquisition, R.R.A.-H. All authors have read and agreed to the published version of the manuscript.

Funding: This project was funded by the Deanship of Scientific Research (DSR) at King Abdulaziz University, Jeddah, under grant no (G-492-130-1442). The authors, therefore, acknowledge with thanks DSR for technical and financial support.

Institutional Review Board Statement: Not applicable.

Informed Consent Statement: Not applicable.

Data Availability Statement: Not applicable.

Conflicts of Interest: The authors declare no conflict of interest.

References

- Lyczak, J.B.; Cannon, C.L.; Pier, G.B. Establishment of *Pseudomonas aeruginosa* infection: Lessons from a versatile opportunist. *Microb. Infect.* **2000**, *2*, 1051–1060. [\[CrossRef\]](#) [\[PubMed\]](#)
- Basseti, M.; Merelli, M.; Temperoni, C.; Astilean, A. New antibiotics for bad bugs: Where are we? *Ann. Clin. Microbiol. Antimicrob.* **2013**, *12*, 22. [\[CrossRef\]](#) [\[PubMed\]](#)
- Tolker-Nielsen, T. *Pseudomonas aeruginosa* biofilm infections: From molecular biofilm biology to new treatment possibilities. *Apmis* **2014**, *122*, 1–51. [\[CrossRef\]](#) [\[PubMed\]](#)
- Nathan, C. Resisting antimicrobial resistance. *Nat. Rev. Microbiol.* **2020**, *18*, 259–260. [\[CrossRef\]](#) [\[PubMed\]](#)
- Reygaert, W.C. An overview of the antimicrobial resistance mechanisms of bacteria. *AIMS Microbiol.* **2018**, *4*, 482. [\[CrossRef\]](#)
- Alharbi, M.G.; Al-Hindi, R.R.; Esmael, A.; Alotibi, I.A.; Azhari, S.A.; Alseghayer, M.S.; Teklemariam, A.D. The “Big Six”: Hidden Emerging Foodborne Bacterial Pathogens. *Trop. Med. Infect. Dis.* **2022**, *7*, 356. [\[CrossRef\]](#)
- Meletis, G. Carbapenem resistance: Overview of the problem and future perspectives. *Ther. Adv. Infect. Dis.* **2016**, *3*, 15–21. [\[CrossRef\]](#)
- Arya, S.S.; Sharma, M.M.; Rookes, J.E.; Cahill, D.M.; Lenka, S.K. Vanilla modulates the activity of antibiotics and inhibits efflux pumps in drug-resistant *Pseudomonas aeruginosa*. *Biologia* **2021**, *76*, 781–791. [\[CrossRef\]](#)
- WHO. *WHO Publishes List of Bacteria for Which New Antibiotics are Urgently Needed*; WHO: Geneva, Switzerland, 2017.
- Zeineldin, M.; Esmael, A.; Al-Hindi, R.R.; Alharbi, M.G.; Ashenafi Bekele, D.; Teklemariam, A.D. Beyond the Risk of Biofilms: An Up-and-Coming Battleground of Bacterial Life and Potential Antibiofilm Agents. *Life* **2023**, *13*, 503. [\[CrossRef\]](#)
- Coronel-Olivares, C.; Reyes-Gómez, L.M.; Hernández-Muñoz, A.; Martínez-Falcón, A.P.; Vázquez-Rodríguez, G.A.; Iturbe, U. Chlorine Disinfection of *Pseudomonas aeruginosa*, Total Coliforms, *Escherichia coli* and *Enterococcus faecalis*: Revisiting Reclaimed Water Regulations. *Water Sci. Technol.* **2011**, *64*, 2151–2157. [\[CrossRef\]](#)
- Watters, C.; DeLeon, K.; Trivedi, U.; Griswold, J.A.; Lyte, M.; Hampel, K.J.; Wargo, M.J.; Rumbaugh, K.P. *Pseudomonas aeruginosa* biofilms perturb wound resolution and antibiotic tolerance in diabetic mice. *Med. Microbiol. Immunol.* **2013**, *202*, 131–141. [\[CrossRef\]](#) [\[PubMed\]](#)
- Høiby, N.; Ciofu, O.; Bjarnsholt, T. *Pseudomonas aeruginosa* biofilms in cystic fibrosis. *Future Microbiol.* **2010**, *5*, 1663–1674. [\[CrossRef\]](#) [\[PubMed\]](#)
- Thi, M.T.T.; Wibowo, D.; Rehm, B.H. *Pseudomonas aeruginosa* biofilms. *Int. J. Mol. Sci.* **2020**, *21*, 8671. [\[CrossRef\]](#) [\[PubMed\]](#)
- Knecht, L.E.; Veljkovic, M.; Fieseler, L. Diversity and function of phage encoded depolymerases. *Front. Microbiol.* **2020**, *10*, 2949. [\[CrossRef\]](#)
- Esmael, A.; Abo-Elmaaty, S.A.; Khafaga, E.M.; Abdelrahman, S.; Hassan, M.G. Efficacy of three lytic bacteriophages for eradicating biofilms of multidrug-resistant *Proteus mirabilis*. *Arch. Virol.* **2021**, *166*, 3311–3322. [\[CrossRef\]](#)
- Jensen, P.Ø.; Givskov, M.; Bjarnsholt, T.; Moser, C. The immune system vs. *Pseudomonas aeruginosa* biofilms. *FEMS Immunol. Med. Microbiol.* **2010**, *59*, 292–305. [\[CrossRef\]](#)
- Sharma, D.; Misba, L.; Khan, A.U. Antibiotics versus biofilm: An emerging battleground in microbial communities. *Antimicrob. Resist. Infect. Control.* **2019**, *8*, 76. [\[CrossRef\]](#)
- Esmael, A.; Hassan, M.G.; Amer, M.M.; Abdelrahman, S.; Hamed, A.M.; Abd-raboh, H.A.; Foda, M.F. Antimicrobial activity of certain natural-based plant oils against the antibiotic-resistant acne bacteria. *Saudi J. Biol. Sci.* **2020**, *27*, 448–455. [\[CrossRef\]](#)
- Tian, F.; Li, J.; Nazir, A.; Tong, Y. Bacteriophage—A promising alternative measure for bacterial biofilm control. *Infect. Drug Resist.* **2021**, *14*, 205. [\[CrossRef\]](#)
- Esmael, A.; Azab, E.; Gobouri, A.A.; Nasr-eldin, M.A.; Moustafa, M.M.A.; Mohamed, S.A.; Badr, O.A.M.; Abdelatty, A.M. Isolation and characterization of two lytic bacteriophages infecting a multi-drug resistant *Salmonella typhimurium* and their efficacy to combat salmonellosis in ready-to-use foods. *Microorganisms* **2021**, *9*, 423. [\[CrossRef\]](#)
- Blundell-Hunter, G.; Enright, M.C.; Negus, D.; Dorman, M.J.; Beecham, G.E.; Pickard, D.J.; Wintachai, P.; Voravuthikunchai, S.P.; Thomson, N.R.; Taylor, P.W. Characterisation of bacteriophage-encoded depolymerases selective for key *Klebsiella Pneumoniae* capsular exopolysaccharides. *Front. Cell. Infect. Microbiol.* **2021**, *11*, 686090. [\[CrossRef\]](#) [\[PubMed\]](#)
- Matsuzaki, S.; Rashel, M.; Uchiyama, J.; Sakurai, S.; Ujihara, T.; Kuroda, M.; Ikeuchi, M.; Tani, T.; Fujieda, M.; Wakiguchi, H. Bacteriophage therapy: A revitalized therapy against bacterial infectious diseases. *J. Infect. Chemother.* **2005**, *11*, 211–219. [\[CrossRef\]](#) [\[PubMed\]](#)
- Soothill, J. Use of bacteriophages in the treatment of *Pseudomonas aeruginosa* infections. *Expert Rev. Anti-Infect. Ther.* **2013**, *11*, 909–915. [\[CrossRef\]](#) [\[PubMed\]](#)
- Abo-Elmaaty, S.A.; Esmael, A.; Bdelrahman, S.; Tarek, E.; Hassan, M.G. Studies on the Application of Bacteriophages and Silver Nanoparticles in The Treatment of *Pseudomonas* spp. *Egypt. Acad. J. Biol. Sci. G. Microbiol.* **2022**, *14*, 23–39. [\[CrossRef\]](#)
- Sulakvelidze, A.; Alavidze, Z.; Morris, J.G. Bacteriophage Therapy. *Antimicrob. Agents Chemother.* **2001**, *45*, 649–659. [\[CrossRef\]](#) [\[PubMed\]](#)

27. Verbeke, G.; De Vos, D.; Vanechoutte, M.; Merabishvili, M.; Zizi, M.; Pirnay, J.-P. European regulatory conundrum of phage therapy. *Future Microbiol.* **2007**, *2*, 485–491. [[CrossRef](#)] [[PubMed](#)]
28. Waters, V.; Grimwood, K. Defining chronic *Pseudomonas aeruginosa* infection in cystic fibrosis. *J. Cyst. Fibros.* **2018**, *17*, 292–293. [[CrossRef](#)]
29. Holguín, A.V.; Rangel, G.; Clavijo, V.; Prada, C.; Mantilla, M.; Gomez, M.C.; Kutter, E.; Taylor, C.; Fineran, P.C.; Barrios, A.F.G. Phage ΦPan70, a putative temperate phage, controls *Pseudomonas aeruginosa* in planktonic, biofilm and burn mouse model assays. *Viruses* **2015**, *7*, 4602–4623. [[CrossRef](#)]
30. Latz, S.; Krüttgen, A.; Häfner, H.; Buhl, E.M.; Ritter, K.; Horz, H.-P. Differential effect of newly isolated phages belonging to PB1-Like, phiKZ-Like and LUZ24-Like Viruses against Multi-Drug Resistant *Pseudomonas aeruginosa* under varying growth conditions. *Viruses* **2017**, *9*, 315. [[CrossRef](#)]
31. Adnan, M.; Shah, M.R.A.; Jamal, M.; Jalil, F.; Andleeb, S.; Nawaz, M.A.; Pervez, S.; Hussain, T.; Shah, I.; Imran, M. Isolation and characterization of bacteriophage to control multidrug-resistant *Pseudomonas aeruginosa* planktonic cells and biofilm. *Biologicals* **2020**, *63*, 89–96. [[CrossRef](#)]
32. Lin, D.M.; Koskella, B.; Lin, H.C. Phage Therapy: An Alternative to Antibiotics in the Age of Multi-Drug Resistance. *World J. Gastrointest. Pharmacol. Ther.* **2017**, *8*, 162–173. [[CrossRef](#)] [[PubMed](#)]
33. Humphries, R.; Bobenchik, A.M.; Hindler, J.A.; Schuetz, A.N. Overview of changes to the clinical and laboratory standards institute performance standards for antimicrobial susceptibility testing, M100. *J. Clin. Microbiol.* **2021**, *59*, e00213-21. [[CrossRef](#)] [[PubMed](#)]
34. Van Twest, R.; Kropinski, A.M. Bacteriophage Enrichment From Water and Soil. *Methods Mol. Biol.* **2009**, *501*, 15–21. [[CrossRef](#)] [[PubMed](#)]
35. Pereira, C.; Silva, Y.J.; Santos, A.L.; Cunha, A.; Gomes, N.C.; Almeida, A. Bacteriophages With Potential for Inactivation of Fish Pathogenic Bacteria: Survival, Host Specificity and Effect on Bacterial Community Structure. *Mar. Drugs* **2011**, *9*, 2236. [[CrossRef](#)]
36. Gencay, Y.E.; Birk, T.; Sørensen, M.C.; Brøndsted, L. Methods for Isolation, Purification, and Propagation of Bacteriophages of *Campylobacter jejuni*. *Methods Mol. Biol.* **2017**, *1512*, 19–28. [[CrossRef](#)]
37. Adams, M.H. *Bacteriophages*; Citeseer: Princeton, NJ, USA, 1959.
38. Teklemariam, A.D.; Alharbi, M.G.; Al-Hindi, R.R.; Alotibi, I.; Aljaddawi, A.A.; Azhari, S.A.; Esmael, A. Isolation and Characterization of Chi-like *Salmonella* Bacteriophages Infecting Two *Salmonella enterica* Serovars, Typhimurium and Enteritidis. *Pathogens* **2022**, *11*, 1480. [[CrossRef](#)]
39. Thung, T.; Siti Norshafawatie, B.; Premarathne, J.; Chang, W.; Loo, Y.; Kuan, C.; New, C.; Ubong, A.; Ramzi, O.; Mahyudin, N. Isolation of food-borne pathogen bacteriophages from retail food and environmental sewage. *Int. Food Res. J.* **2017**, *24*, 450–454.
40. Jurczak-Kurek, A.; Gašior, T.; Nejman-Faleńczyk, B.; Bloch, S.; Dydecka, A.; Topka, G.; Necel, A.; Jakubowska-Deredas, M.; Narajczyk, M.; Richert, M.; et al. Biodiversity of Bacteriophages: Morphological and Biological Properties of a Large Group of Phages Isolated From Urban Sewage. *Sci. Rep.* **2016**, *6*, 34338. [[CrossRef](#)]
41. Verma, V.; Harjai, K.; Chhibber, S. Characterization of a T7-like Lytic Bacteriophage of *Klebsiella pneumoniae* B5055: A Potential Therapeutic Agent. *Curr. Microbiol.* **2009**, *59*, 274–281. [[CrossRef](#)]
42. Wang, Z.; Zheng, P.; Ji, W.; Fu, Q.; Wang, H.; Yan, Y.; Sun, J. SLPW: A Virulent Bacteriophage Targeting Methicillin-Resistant *Staphylococcus aureus* In Vitro and In Vivo. *Front. Microbiol.* **2016**, *7*, 934. [[CrossRef](#)]
43. Liu, J.; Gao, S.; Dong, Y.; Lu, C.; Liu, Y. Isolation and characterization of bacteriophages against virulent *Aeromonas hydrophila*. *BMC Microbiol.* **2020**, *20*, 141. [[CrossRef](#)] [[PubMed](#)]
44. Le, S.; Yao, X.; Lu, S.; Tan, Y.; Rao, X.; Li, M.; Jin, X.; Wang, J.; Zhao, Y.; Wu, N.C. Chromosomal DNA deletion confers phage resistance to *Pseudomonas aeruginosa*. *Sci. Rep.* **2014**, *4*, 4738. [[CrossRef](#)] [[PubMed](#)]
45. Othman, A.M.; Esmael, A.; Abdelrahman, S.; Shraf, A.; Hassan, M.G. Biocontrol of *Acinetobacter baumannii*-S-MH Using Bacteriophages Isolated from Sewage Water. *Egypt Acad. J. Biol. Sci. G. Microbiol.* **2021**, *13*, 17–32. [[CrossRef](#)]
46. Valentine, R.C.; Shapiro, B.; Stadtman, E. Regulation of glutamine synthetase. XII. Electron microscopy of the enzyme from *Escherichia coli*. *Biochemistry* **1968**, *7*, 2143–2152. [[CrossRef](#)] [[PubMed](#)]
47. Ackermann, H.-W.; DuBow, M.; Jarvis, A.; Jones, L.; Krylov, V.; Maniloff, J.; Rocourt, J.; Safferman, R.; Schneider, J.; Seldin, L. The species concept and its application to tailed phages. *Arch. Virol.* **1992**, *124*, 69–82. [[CrossRef](#)]
48. Di Domenico, E.G.; Toma, L.; Provot, C.; Ascenzioni, F.; Sperduti, I.; Prignano, G.; Gallo, M.T.; Pimpinelli, F.; Bordignon, V.; Bernardi, T. Development of an in vitro assay, based on the Biofilm Ring Test[®], for rapid profiling of biofilm-growing bacteria. *Front. Microbiol.* **2016**, *7*, 1429. [[CrossRef](#)]
49. Fong, S.A.; Drilling, A.; Morales, S.; Cornet, M.E.; Woodworth, B.A.; Fokkens, W.J.; Psaltis, A.J.; Vreugde, S.; Wormald, P.-J. Activity of bacteriophages in removing biofilms of *Pseudomonas aeruginosa* isolates from chronic rhinosinusitis patients. *Front. Cell. Infect. Microbiol.* **2017**, *7*, 418. [[CrossRef](#)]
50. Arya, S.S.; Sharma, M.M.; Das, R.K.; Rookes, J.; Cahill, D.; Lenka, S.K. Vanillin mediated green synthesis and application of gold nanoparticles for reversal of antimicrobial resistance in *Pseudomonas aeruginosa* clinical isolates. *Heliyon* **2019**, *5*, e02021. [[CrossRef](#)]
51. Relucenti, M.; Familiari, G.; Donfrancesco, O.; Taurino, M.; Li, X.; Chen, R.; Artini, M.; Papa, R.; Selan, L. Microscopy methods for biofilm imaging: Focus on SEM and VP-SEM pros and cons. *Biology* **2021**, *10*, 51. [[CrossRef](#)]

52. Yazdi, M.; Bouzari, M.; Ghaemi, E.A.; Shahin, K. Isolation, characterization and genomic analysis of a novel bacteriophage VB_EcoS-Golestan infecting multidrug-resistant *Escherichia coli* isolated from urinary tract infection. *Sci. Rep.* **2020**, *10*, 7690. [[CrossRef](#)]
53. Stothard, P.; Wishart, D.S. Circular genome visualization and exploration using CGView. *Bioinformatics* **2005**, *21*, 537–539. [[CrossRef](#)] [[PubMed](#)]
54. Lavigne, R.; Sun, W.; Volckaert, G. PHIRE, a deterministic approach to reveal regulatory elements in bacteriophage genomes. *Bioinformatics* **2004**, *20*, 629–635. [[CrossRef](#)] [[PubMed](#)]
55. Sullivan, M.J.; Petty, N.K.; Beatson, S.A. Easyfig: A genome comparison visualizer. *Bioinformatics* **2011**, *27*, 1009–1010. [[CrossRef](#)] [[PubMed](#)]
56. Besemer, J.; Borodovsky, M. GeneMark: Web software for gene finding in prokaryotes, eukaryotes and viruses. *Nucleic Acids Res.* **2005**, *33*, W451–W454. [[CrossRef](#)]
57. Zhou, Y.; Liang, Y.; Lynch, K.H.; Dennis, J.J.; Wishart, D.S. PFAST: A fast phage search tool. *Nucleic Acids Res.* **2011**, *39*, W347–W352. [[CrossRef](#)]
58. Altschul, S.F.; Madden, T.L.; Schäffer, A.A.; Zhang, J.; Zhang, Z.; Miller, W.; Lipman, D.J. Gapped BLAST and PSI-BLAST: A new generation of protein database search programs. *Nucleic Acids Res.* **1997**, *25*, 3389–3402. [[CrossRef](#)]
59. Chan, P.P.; Lowe, T.M. GtRNAdb: A database of transfer RNA genes detected in genomic sequence. *Nucleic Acids Res.* **2009**, *37*, D93–D97. [[CrossRef](#)]
60. Schattner, P.; Brooks, A.N.; Lowe, T.M. The tRNAscan-SE, snoscan and snoGPS web servers for the detection of tRNAs and snoRNAs. *Nucleic Acids Res.* **2005**, *33*, W686–W689. [[CrossRef](#)]
61. Chen, L.; Xiong, Z.; Sun, L.; Yang, J.; Jin, Q. VFDB 2012 update: Toward the genetic diversity and molecular evolution of bacterial virulence factors. *Nucleic Acids Res.* **2012**, *40*, D641–D645. [[CrossRef](#)]
62. Kleinheinz, K.A.; Joensen, K.G.; Larsen, M.V. Applying the ResFinder and VirulenceFinder web-services for easy identification of acquired antibiotic resistance and *E. coli* virulence genes in bacteriophage and prophage nucleotide sequences. *Bacteriophage* **2014**, *4*, e27943. [[CrossRef](#)]
63. Katoh, K.; Rozewicki, J.; Yamada, K.D. MAFFT online service: Multiple sequence alignment, interactive sequence choice and visualization. *Brief. Bioinform.* **2019**, *20*, 1160–1166. [[CrossRef](#)] [[PubMed](#)]
64. Letunic, I.; Bork, P. Interactive tree of life (iTOL) v3: An online tool for the display and annotation of phylogenetic and other trees. *Nucleic Acids Res.* **2016**, *44*, W242–W245. [[CrossRef](#)] [[PubMed](#)]
65. Darzentas, N. Circoletto: Visualizing sequence similarity with Circos. *Bioinformatics* **2010**, *26*, 2620–2621. [[CrossRef](#)] [[PubMed](#)]
66. Hu, Y.-Y.; Cao, J.-M.; Yang, Q.; Chen, S.; Lv, H.-Y.; Zhou, H.-W.; Wu, Z.; Zhang, R. Risk factors for carbapenem-resistant *Pseudomonas aeruginosa*, Zhejiang Province, China. *Emerg. Infect. Dis.* **2019**, *25*, 1861. [[CrossRef](#)] [[PubMed](#)]
67. Han, J.E.; Kim, J.H.; Hwang, S.Y.; Choresca Jr, C.H.; Shin, S.P.; Jun, J.W.; Chai, J.Y.; Park, Y.H.; Park, S.C. Isolation and characterization of a Myoviridae bacteriophage against *Staphylococcus aureus* isolated from dairy cows with mastitis. *Res. Vet. Sci.* **2013**, *95*, 758–763. [[CrossRef](#)]
68. Kwiatek, M.; Parasion, S.; Mizak, L.; Gryko, R.; Bartoszcze, M.; Kocik, J. Characterization of a bacteriophage, isolated from a cow with mastitis, that is lytic against *Staphylococcus aureus* strains. *Arch. Virol.* **2012**, *157*, 225–234. [[CrossRef](#)]
69. Zanetti, C.; Mingrone, R.; Kisielius, J.; Ueda-Ito, M.; Pignatari, A.C.C. Characterization of bacteriophages infecting clinical isolates of *Pseudomonas aeruginosa* stored in a culture collection. *Braz. J. Med. Biol. Res.* **2013**, *46*, 689–695. [[CrossRef](#)]
70. Jamal, M.; Andleeb, S.; Jalil, F.; Imran, M.; Nawaz, M.A.; Hussain, T.; Ali, M.; Das, C.R. Isolation and characterization of a bacteriophage and its utilization against multi-drug resistant *Pseudomonas aeruginosa*-2995. *Life Sci.* **2017**, *190*, 21–28. [[CrossRef](#)]
71. Piracha, Z.; Saeed, U.; Khurshid, A.; Chaudhary, W.N. Isolation and partial characterization of virulent phage specific against *Pseudomonas aeruginosa*. *Glob. J. Med. Res.* **2014**, *14*, 1–8.
72. Klai, N.; Sellamuthu, B. Bacteriophages isolated from hospital wastewater and its role in controlling drug-resistant pathogens. In *Current Developments in Biotechnology and Bioengineering*; Elsevier: Amsterdam, The Netherlands, 2020; pp. 327–376.
73. White, R.; Chiba, S.; Pang, T.; Dewey, J.S.; Savva, C.G.; Holzenburg, A.; Pogliano, K.; Young, R. Holin triggering in real time. *Proc. Natl. Acad. Sci. USA* **2011**, *108*, 798–803. [[CrossRef](#)]
74. Wang, I.-N.; Smith, D.L.; Young, R. Holins: The protein clocks of bacteriophage infections. *Annu. Rev. Microbiol.* **2000**, *54*, 799–825. [[CrossRef](#)] [[PubMed](#)]
75. Bailly-Bechet, M.; Vergassola, M.; Rocha, E. Causes for the intriguing presence of tRNAs in phages. *Genome Res.* **2007**, *17*, 1486–1495. [[CrossRef](#)] [[PubMed](#)]
76. Jain, R.; Rivera, M.C.; Lake, J.A. Horizontal gene transfer among genomes: The complexity hypothesis. *Proc. Natl. Acad. Sci. USA* **1999**, *96*, 3801–3806. [[CrossRef](#)] [[PubMed](#)]
77. Wilson, J.H. Function of the bacteriophage T4 transfer RNA's. *J. Mol. Biol.* **1973**, *74*, 753–757. [[CrossRef](#)]
78. Fister, S.; Robben, C.; Witte, A.K.; Schoder, D.; Wagner, M.; Rossmann, P. Influence of environmental factors on phage–bacteria interaction and on the efficacy and infectivity of phage P100. *Front. Microbiol.* **2016**, *7*, 1152. [[CrossRef](#)]
79. Hazem, A. Effects of temperatures, pH-values, ultra-violet light, ethanol and chloroform on the growth of isolated thermophilic *Bacillus* phages. *New Microbiol.* **2002**, *25*, 469–476.

80. Smolarska, A.; Rabalski, L.; Narajczyk, M.; Czajkowski, R. Isolation and phenotypic and morphological characterization of the first Podoviridae lytic bacteriophages ϕ A38 and ϕ A41 infecting *Pectobacterium parmentieri* (former *Pectobacterium wasabiae*). *Eur. J. Plant Pathol.* **2018**, *150*, 413–425. [[CrossRef](#)]
81. Fan, N.; Qi, R.; Yang, M. Isolation and characterization of a virulent bacteriophage infecting *Acinetobacter johnsonii* from activated sludge. *Res. Microbiol.* **2017**, *168*, 472–481. [[CrossRef](#)]
82. Abedon, S.T.; Kuhl, S.J.; Blasdel, B.G.; Kutter, E.M. Phage treatment of human infections. *Bacteriophage* **2011**, *1*, 66–85. [[CrossRef](#)]
83. Moldovan, R.; Chapman-McQuiston, E.; Wu, X. On kinetics of phage adsorption. *Biophys. J.* **2007**, *93*, 303–315. [[CrossRef](#)]
84. Guo, Y.; Chen, P.; Lin, Z.; Wang, T. Characterization of two *Pseudomonas aeruginosa* viruses vB_PaeM_SCUT-S1 and vB_PaeM_SCUT-S2. *Viruses* **2019**, *11*, 318. [[CrossRef](#)] [[PubMed](#)]
85. Vukotic, G.; Obradovic, M.; Novovic, K.; Di Luca, M.; Jovicic, B.; Fira, D.; Neve, H.; Kojic, M.; McAuliffe, O. Characterization, antibiofilm, and depolymerizing activity of two phages active on carbapenem-resistant *Acinetobacter baumannii*. *Front. Med.* **2020**, *7*, 426. [[CrossRef](#)] [[PubMed](#)]
86. Oliveira, V.C.; Bim, F.L.; Monteiro, R.M.; Macedo, A.P.; Santos, E.S.; Silva-Lovato, C.H.; Paranhos, H.F.; Melo, L.D.; Santos, S.B.; Watanabe, E. Identification and characterization of new bacteriophages to control multidrug-resistant *Pseudomonas aeruginosa* biofilm on endotracheal tubes. *Front. Microbiol.* **2020**, *11*, 580779. [[CrossRef](#)] [[PubMed](#)]
87. Yuan, Y.; Qu, K.; Tan, D.; Li, X.; Wang, L.; Cong, C.; Xiu, Z.; Xu, Y. Isolation and Characterization of a Bacteriophage and Its Potential to Disrupt Multi-Drug Resistant *Pseudomonas aeruginosa* Biofilms. *Microb. Pathog.* **2019**, *128*, 329–336. [[CrossRef](#)]
88. Volozhantsev, N.V.; Shpirt, A.M.; Borzilov, A.I.; Komisarova, E.V.; Krasilnikova, V.M.; Shashkov, A.S.; Verevkin, V.V.; Knirel, Y.A. Characterization and therapeutic potential of bacteriophage-encoded polysaccharide depolymerases with β galactosidase activity against *Klebsiella Pneumoniae* K57 capsular type. *Antibiotics* **2020**, *9*, 732. [[CrossRef](#)]

Disclaimer/Publisher's Note: The statements, opinions and data contained in all publications are solely those of the individual author(s) and contributor(s) and not of MDPI and/or the editor(s). MDPI and/or the editor(s) disclaim responsibility for any injury to people or property resulting from any ideas, methods, instructions or products referred to in the content.